A CONSTITUTIONAL STUDY OF A DUAL PHASE STEEL CONTAINING 12% CHROMIUM

by
G.B. Schaffer

A thesis submitted to the Faculty of Engineering, University of Cape Town in fulfilment of the degree of Master of Science in Applied Science.

Department of Metallurgy and Materials Science,
University of Cape Town.

March 1983

ACKNOWLEDGEMENTS

I would like to thank the following people who assisted me in the research work.

Professor A. Ball for his help and advice.

Mr J.J. Ward for his interest in and advice with the metallography.

Dr D. Crawford and Mr D. Gerneke for help with the electron microscope.

Mr N. Dreze and Mr A. Rapley for technical assistance.

Mr B. Greeves for his photographic expertise.

Mrs E.L. Diamond for the preparation of the manuscript.

Middelburg Steel and Alloys (Pty) Ltd for financial support.

ABSTRACT

This thesis involved a study of the phase transformations in a chromium containing corrosion resistant dual phase steel, designated 3CR12. The objectives included the determination of time-temperature-transformation (TTT) diagrams for the transformations between austenite and ferrite and an investigation into the factors controlling these reactions. The austenite decomposition reaction for a high nickel alloy, 3CR12Ni, and the effect of varying titanium concentrations on the equilibrium phases present in 3CR12, were also examined.

Dilatometry was used to determine the transformation temperatures between austenite and ferrite and the Ms temperatures for the alloys investigated. The kinetics of the reactions were investigated by optical microscopy using two different etching techniques while the volume fractions of the various constituents were determined by a point counting method. Transmission electron microscopy was used to study the carbide morphologies and the nucleation and growth modes of the phases during the transformations. The distribution of the alloy elements were determined by microhardness measurements, an electronprobe microanalysis and a Kevex spectrometer attached to a scanning electron microscope.

The 3CR12 alloy used in this study did not become fully austenitic above the Ae_3; it lies in the nose of the gamma loop of the Fe-Cr phase diagram. Two temperature regimes were identified on the decomposition of austenite. At 750^{o}C the existing ferrite grains grew into the austenite matrix, while at 650^{o}C and 700^{o}C new ferrite was sympathetically nucleated i.e. it was heterogeneously nucleated on existing ferrite/austenite grain boundaries. Two types of carbide morphologies were formed. These were random precipitation within the ferrite grains and interphase precipitation. The TTT diagram showed conventional "C" curve kinetics.

The austenitisation reaction occurred by a para-equilibrium mechanism. The rate controlling process was the structural change

from ferrite to austenite; the reaction was not long range diffusion controlled. The speed of the reaction increased continuously with increasing transformation temperature.

No growth of ferrite occurred on isothermal transformation of 3CR12Ni at temperatures below the Ae_1.

Increasing the bulk titanium content increased the Ms, Ae_1 and Ae_3 temperatures of 3CR12 due to the removal of carbon from, and the addition of titanium to, solution.

CONTENTS

CHAPTER 1 : INTRODUCTION

1.1 A chromium containing corrosion resistant steel

Market research undertaken for Middelburg Steel and Alloys (Pty) Ltd (formerly Southern Cross Steel) had indicated an escalating need for a corrosion resistant steel which could possibly replace mild steel for use in mildly corrosive environments. Besides improved corrosion resistance, such a steel should have similar mechanical properties and welding characteristics to mild steel while remaining cost-effective. The cost benefit must be calculated on the basis of the increased cost of corrosion protection, maintenance and production downtime needed for mild steel, versus the higher cost of the new material resulting from the addition of expensive alloying elements. The relative abundance of chrome ore in Southern Africa, plus a large potential market, meant a program to develop such a steel was economically feasible.

Middelburg Steel has therefore developed a twelve percent chromium steel from the ferritic AISI 409. This steel, designated 3CR12, has a very low carbon content, minor nickel and manganese additions and is titanium stabilised. After an intercritical anneal this steel has a duplex martensite/ferrite microstructure similar to the low alloy steels currently being developed for use in the automotive industry. After an initial research program, the steel was tested in prototype form in eighty-one different applications ranging from chute liners in the mining industry to heat exchangers in the chemical industry (Melvill et al, 1980). In 1978, 3CR12 became commercially available in plate form, varying in thickness between 3 and 32 mm. It is in use as electrification masts for the South African Railways and has seen extensive service in the mining industry for materials handling purposes (Walker, 1982).

The research program, however, is continuing with the aim of improving the in-service performance of 3CR12 by optimising the com-

position and microstructure through careful design of the manufacturing process.

1.2 Dual phase steels

Following the Middle East conflict of 1973 and the resulting energy crisis, a need was established for the production of more fuel-efficient automobiles. One of the quickest and cheapest ways of reducing fuel consumption was to reduce the overall weight of the car by changing the materials used in its construction. To this end, Hayami and Furakawa, in 1975, published a comprehensive description of microduplex steels, which led to the commercial development of dual phase steels for use in car bodies (Owen, 1980).

The microstructure of dual phase steels consists of islands of martensite in a ferrite matrix. This is formed by either controlled cooling during and after rolling or by an intercritical anneal subsequent to cold rolling. This microstructure allows the use of thinner gauge material which has the same strength as the conventional high strength low alloy (HSLA) steels but with much greater ductility. It is thus possible to create a high strength steel without sacrificing formability.

The martensite volume fraction is usually standardised at 0,2 and occurs as isolated islands in the ferrite matrix. The interelationships between the microconstituents, martensite and ferrite, gives the steel continuous yielding characteristics (e.g. Davies, 1978) with a high strain hardening coefficient, n. High n values are a measure of the steel's resistance to necking and hence dual phase steels show uniform strain distribution and the elimination of stretcher strains which form during cold working operations. Tensile fracture occurs by the nucleation of voids at small inclusions and at the ferrite/martensite interface (e.g. Marder, 1982). This does not occur until the microconstituents are deformed and highly strained (Rashid, 1981). Final fracture results from void coalescence.

1.3 Objectives

In this section some of the problems associated with the production of 3CR12 are discussed and the objectives of this dissertation are outlined.

1.3.1 Kinetics of phase transformations A metallurgical phase diagram gives information on which phases will be present in an alloy system when it is at thermodynamic equilibrium. However, it does not illustrate any kinetic effects or the presence of metastable phases such as martensite. It was not until 1930 when Davenport and Bain initiated the isothermal transformation technique that time-temperature-transformation (TTT) diagrams became a recognised method of describing the kinetics of phase changes. This technique involves quenching a specimen from some initial transformation temperature to a lower, predetermined temperature and monitoring the course of the transformation by measuring a physical property such as length or by removing specimens after fixed time intervals, quenching into water and determining the extent of the reaction metallographically. In this manner a diagram can be constructed which illustrates the effect of time on a phase transformation.

Such a diagram can then be used for the design of a heat treatment to optimise the microstructure of a material enabling specific mechanical, physical and chemical properties to be attained. These diagrams can also be used as a guide in the manufacturing process to control cooling rates during rolling if no subsequent heat treatment is utilized. Similarly the reverse transformation, that is, the upquenching to a higher hold temperature, can provide kinetic data to facilitate the design of an intercritical anneal during the manufacture of dual phase steels.

One of the objectives of this dissertation was to construct isothermal transformation diagrams for both transformations, i.e. to and from austenite, for 3CR12, and to investigate the factors

controlling these reactions. The austenite decomposition reaction for a 3CR12 alloy with a nominally higher nickel content, 3CR12Ni, was also examined. Although it is recognised that laboratory determined diagrams do not necessarily model the manufacturing process accurately, they can provide a guide for the production of 3CR12.

1.3.2 Titanium The precipitation of chromium carbide and the subsequent depletion of chrome from the surrounding matrix occurs when stainless steel is held for appreciable times at about 700^{o}C. This depletion often occurs, for example, in a narrow band on either side of a weld and significantly reduces the corrosion resistance in this zone. This can be prevented by stabilising the steel with titanium or niobium since they have a greater affinity for carbon than chrome has. Titanium/niobium carbides are formed in preference to chrome carbides, which leaves chromium in solution and the steel retains its corrosion resistance. As one of the design criteria for 3CR12 was good weldability, it was necessary to stabilise the steel with titanium.

The addition of titanium, however, may alter the equilibrium phases present in 3CR12 by reducing the free carbon content and also through the presence of any uncombined titanium. Since varying titanium contents might significantly alter the microstructure of 3CR12 after a normal production run, an investigation was conducted into the effect of titanium on the equilibrium phases present in 3CR12.

CHAPTER 2 : LITERATURE SURVEY

2.1 The austenite decomposition reaction

2.1.1 Introduction When austenite is cooled from its thermodynamically stable temperature range, it must transform to one or more new phases. This can occur by two different mechanisms: (a) nucleation and growth or (b) martensitic. The latter reaction will be discussed in Section 2.4. Characteristics of the nucleation and growth reaction (after Christian, 1975) are: (a) The amount of transformation increases with increasing time until a state of minimum free energy is reached; (b) the transformation depends on temperature in that the equilibrium state is itself a function of temperature. If given sufficient time, the transformation will continue until complete. The velocity of the transformation varies considerably with temperature. (c) The individual atoms move independently of each other. The composition of the reaction products need not be related in any way to those of the original phase.

The transformation from austenite by nucleation and growth can result in a number of different phases, depending on the alloy composition, the reaction temperature and the time for which it is allowed to proceed. The following discussion will be limited to the formation of proeutectoid ferrite and ferrite with associated carbides.

2.1.2 Morphology of proeutectoid ferrite Proeutectoid ferrite may be regarded, in a general sense, as a precipitate crystal growing in a matrix of different structure and composition. The principle factors responsible for the precipitate morphology are; (a) the nature of the site at which a precipitate crystal nucleates and (b) the growth characteristics of the interphase boundary

separating the precipitate from the matrix (Aaronson et al, 1970). These factors are general in nature and do not depend on specific alloy system characteristics, such as the crystal structure of the two phases and the identity of the solute and solvent atoms. The morphological classification system of these precipitates consists of four principle categories (Dubé, 1948). These are (a) grain boundary allotriomorphs which nucleate at grain boundaries in the matrix phase and grow along them, (b) side-plates which grow into the matrix from an allotriomorph, (c) intragranular plates which form in the interior of a matrix grain and (d) equiaxed intragranular idiomorphs which form in matrix grain interiors.

Honeycombe (1976) suggests that at transformation temperatures above 700^{o}C, nucleation of ferrite takes place predominantly at the austenite grain boundaries because these are both energetically favourable nucleation sites and provide faster paths for diffusion. Ricks et al (1981) have found equiaxed ferrite allotriomorphs and Widmanstätten ferrite in an Fe-7,4% Cr-1,8% Ni alloy isothermally reacted between 600 and 660^{o}C. The Widmanstätten ferrite could be either plate like or saw teeth and either primary (i.e. grown from a grain boundary) or secondary (i.e. grown from an existing allotriomorph). Aaronson and Wells (1956) reported the nucleation of proeutectoid ferrite at ferrite-austenite boundaries in an Fe-0,39% C-0,76% Mn alloy. They called this phenomenon sympathetic nucleation and also noted similar effects on different alloy systems which were reported by other authors.

2.1.3 Kinetics As discussed in Section 1.3.1, the kinetics of a phase change can be illustrated by a TTT diagram. For plain carbon steels the TTT curve for the decomposition of austenite has a simple, well-defined "C" shape. The nose of the curve represents the temperature at which the reaction proceeds most rapidly, slowing down at higher and lower temperatures. The reasons for this shape are due to the interaction of the

thermodynamic driving force governing the reaction and the diffusivity of carbon. At high temperatures the driving force is low but the diffusivity of carbon is high, whereas at low temperatures these effects are reversed. At intermediate temperatures, i.e. in the nose portion of the curve, the driving force and diffusion rate are optimised and the maximum reaction rate is achieved.

In general, the proeutectoid ferrite reaction for alloy steels show similar "C" curve kinetics, although the nose of the curve may be displaced to shorter or longer times. The addition of 12% Cr to a low carbon steel retards the ferrite reaction and the steel becomes air hardened (Irvine et al, 1979). The addition of 1% Ni to this steel retards the reaction further so that the onset of ferrite formation occurs after one hour at $700^{o}C$. Coldren and Eldis (1980) found that increasing the chrome content of a low alloy steel from 0% to 0,48% retarded the ferrite start reaction by a factor of ten, whereas increasing the molybdenum content by the same amount retarded the reaction by a lesser extent. Additions of up to 7% Ni to an Fe-2% Cu alloy significantly retards the reaction kinetics (Ricks et al, 1979). The addition of most other common alloying elements show similar effects (Honeycombe, 1981). These elements retard the proeutectoid ferrite growth kinetics because they have lower diffusivities and also reduce the rate of diffusion of carbon in iron (Honeycombe, 1979). However, Al, Si and Co displace the TTT curve for the initiation of proeutectoid ferrite to shorter reaction times relative to Fe-C alloys (Kinsman and Aaronson, 1973). The increased rates of nucleation and growth due to these elements is a result of the increase in driving force which they provide.

2.1.4 The partitioning of alloying elements The relevant phase diagrams show that austenite and ferrite can dissolve different quantities of the various alloying elements. At equilibrium therefore, the alloying elements should partition

between the two phases. It is thus feasible that these elements may control the rate of transformation from austenite to ferrite. Since the rate of carbon diffusion is more rapid than that of the substitutional elements, it is possible that the latter may control the reaction kinetics in Fe-C-X alloys, where X is Cr, Ni, Mn etc.

In 1966, Aaronson and Domian published their results of an electronprobe analysis into the partitioning of a number of alloying elements between austenite and proeutectoid ferrite in Fe-C-X alloys. They found there was no partitioning of Si, Mo, Co, Al, Cr and Cu between austenite and ferrite during the early stages of the transformation at any temperature. Partitioning did occur for Ni, Mn and Pt steels above a characteristic critical temperature. There were no significant concentration profiles in the ferrite but there were often unequal concentrations of nickel on either side of an austenite grain. They found that the growth kinetics of proeutectoid ferrite was controlled by alloying element diffusion when partitioning occurred and by carbon diffusion when it did not.

Aaronson et al (1966) calculated a no-partition Ae_3 curve which follows a temprature-composition path lying below the equilibrium Ae_3 curve. At isothermal transformation temperatures lying between these curves, the occurrence of partitioning is a thermodynamic prerequisite for the formation of proeutectoid ferrite. At temperatures below the no-partition Ae_3 curve, the precipitation of ferrite without partitioning is thermodynamically permissible. Only the no-partition $\gamma/\gamma + \alpha$ curves for Fe-C-Mn and Fe-C-Ni fall substantially below the equilibrium Ae_3 curve. They suggested that the partitioning effect noted in the Ni and Mn steels is due to the no-partition curve lying sufficiently below the equilibrium Ae_3 curve, thus allowing adequate undercooling to occur in this region, so that partitioned ferrite can grow at observable rates. From the nature of the nickel

concentration gradients they concluded that the growth of partitioned ferrite is controlled by the diffusion of alloying elements in the austenite. The reason for slower growth in Fe-C-X alloys where X does not partition and Fe-C alloys is due to the X atoms collecting on the γ/α boundary and exerting a solute drag effect (Honeycombe, 1981) and to the lower diffusivity of carbon resulting from the addition of X.

Hultgren (1947) proposed a third mechanism for the growth of proeutectoid ferrite. The alloying element X and the solvent participate in the change in crystal structure only and their ratio is held constant across the phase boundary. The boundary exists in a state of para-equilibrium. The growth kinetics are controlled by carbon diffusion. For the no-partition case, Coates (1973) proposed that the initial growth period immediately following nucleation may be entirely interface controlled with neither C nor X in local equilibrium. This will be of short duration and the precipitate soon grows via the para-equilibrium mode. After a certain growth period the interface will depart from this state, pass through an infinity of thermodynamically undefined non-equilibrium states and ultimately arrive at local equilibrium.

2.1.5 Interphase precipitation Isothermally transformed alloy steels can possess microstructures which are midway between the two classical eutectoid structures, viz. proeutectoid ferrite and pearlite. At low magnifications the microstructure appears to be fully ferritic, whereas high resolution electron microscopy reveals fine alloy carbides. There are three major carbide morphologies (after Honeycombe, 1981): (a) The alloy carbides form fine fibres or laths which grow normal to the γ/α interface as the ferrite moves into the austenite matrix; (b) precipitation of carbides on dislocations in supersaturated ferrite; (c) carbides precipitate on the γ/α interface which then moves to a new position where the nucleation process begins again, resulting

in a fine banded dispersion of carbides parallel to the γ/α interface.

The interphase precipitation phenomenon has been widely reported eg. Berry and Honeycombe (1970), Davenport and Honeycombe (1971), Batte and Honeycombe (1973) and Heikkinen (1973), while Honeycombe (1976) presented a detailed review. The major findings are: (a) many alloy carbides adopt this morphology e.g. VC, TiC, Cr_7C_3, $Cr_{23}C_6$ and Mo_2C as well as complex alloy carbonitrides. (b) The carbide size is usually less than 10μm while the band spacing can vary from 5μm to greater than 50μm. Both the carbide size and band spacing increase with increasing transformation temperature and decreasing volume fraction of carbide. They also increase with the addition of alloying elements such as Ni and Mn, which retard the nucleation and growth of ferrite. (c) The precipitates frequently develop on only one of the possible Widmanstätten varients. (d) Interphase precipitation is predominantly associated with ferrite growing by ledge migration. The carbides nucleate on the low energy, non-mobile planar faces of the γ/α interface and grow into the ferrite.

2.2 The austenitisation reaction

2.2.1 Introduction Since the formation of austenite often forms part of the steel heat treatment cycle, the reaction has significant commercial applicability even though the austenite decomposes to other transformation products on cooling. However, the initial austenite condition determines the microstructure and mechanical properties of the final product. The austenitisation reaction is particularly important during the manufacture of dual phase steels since it controls the morphology and distribution of the martensite. Although there are many similarities between the

austenite formation and decomposition reactions, the one is not simply a reversal of the other.The austenitisation reaction is affected by a number of variables, namely the starting structure, alloy composition, reaction temperature and heating rate.

2.2.2 Kinetics The kinetics of the austenite decomposition and formation reactions are very different. In contrast to the decomposition kinetics, as discussed in Section 2.1.3, during the formation of austenite on heating, both the thermodynamic driving force and the diffusion rate increase with increasing temperature and therefore the reaction rate increases continuously with increasing temperature. "C" curve kinetics are seldom obtained (Law and Edmonds, 1980). Lenel (1980), however, found "C" curve kinetics for an Fe-12% Cr-0,2% C alloy and an Fe-1,2% Mn-0,1% C alloy austenitised in the two phase austenite plus ferrite region and showed that this was due to impingement of neighbouring austenite grains and their respective diffusion fields.

The rate of nucleation and growth of austenite has generally been found to be sensitive to the starting structure and heating rate. This was first shown by Roberts and Mehl (1943) while Law and Edmonds (1980) showed that austenitisation is significantly faster in the order martensite>bainite>ferrite. The rate of formation of austenite increases with increasing heating rate (Speich and Szirmae, 1969). Plitcha and Aaronson (1974) studied the growth of austenite into a martensite matrix. They found (a) Mo and Cr retard the austenite growth kinetics due to solute drag effects; (b) Mn, Ni and Cu increase the driving force for both nucleation and growth due to the lower temperature range of the no-partition Ae_3 and hence the kinetics are enhanced and (c) Si, Al and Co decrease the driving force but increase the kinetics for austenite formation and hence the overall kinetics are intermediate between (a) and (b) type elements.

2.2.3 Morphology Fong and Glover (1975) studied the crystallographic relationships in the precipitation of austenite at ferrite grain boundaries during the nitriding of a ferrite Fe-1,93% Mn material. They categorised the various austenite morphologies on the basis of Aaronson's modification of Dubé's classification of proeutectoid ferrite. They concluded that (a) when austenite nucleated with an approximate Kurdjimov-Sachs relationship with one ferrite grain, the austenite grew into the ferrite grain with which it had no crystallographic relationship, (b) when austenite nucleated with an approximate Kurdjimov-Sachs relationship with both ferrite grains, a primary sideplate morphology resulted and (c) when there was no special crystallographic relationship with either ferrite grain, the austenite grew with an allotriomorphic or idiomorphic morphology.

Pavlick et al (1966) found that the morphology of austenite growing into ferrite can be systematically changed by the addition of V, Cr, Si, Ti and Al to zone refined iron. These elements caused preferential grain boundary penetration with a reduction of growth into the adjacent grains. They also caused the austenite/ferrite interface to become more ragged. Ni, Co, Mn and Mo had no significant morphological effect.

When other starting structures are used, e.g. martensite, pearlite or ferrite with spheroidised cementite, different austenite morphologies can result. This is due to the austenite nucleating at different sites e.g. at boundaries of ferrite and carbide or at adjacent pearlite colonies (Speich and Szirmae 1969). This is supported by Molinder (1956), Nemoto (1977) and Hillert et al (1971) who reported the envelopment of a cementite spheroid by austenite which then grew into the surrounding ferrite. It is not known whether fine alloy carbides inherit the role of cementite in the nucleation of austenite (Law and Edmonds, 1980). Plitcha and Aaronson (1974) found that austenite grew as allotriomorphs and idiomorphs along prior austenite grain boundaries and formed an acicular structure along martensite lath boundaries which lay

within prior austenite grains.

2.2.4 Mechanism Matsuda and Okamura (1974, a,b) using a martensitic starting structure, found that acicular austenite grains were formed by a reverse martensitic transformation. They based this conclusion on the morphology of the austenite grains and the crystallographic relationship they had with the original martensite. Albutt and Garber (1966) found that at very high heating rates (> $500^{o}C$/sec) there was evidence for a diffusionless ferrite to austenite transformation. They suggested that it might be due to a shear mechanism although the relevant crystallographic data was not determined. Speich and Szirmae (1969) suggest that the ferrite to austenite transformation in a low carbon, Fe-C alloy, occurs by a massive transformation at heating rates of $10^{6^{o}}C$/sec. Many other studies, e.g. Roberts and Mehl (1943), Grozier et al (1965), Garcia and De Ardo (1979) and Wycliffe et al (1981) have shown that the formation of austenite occurs by a nucleation and growth process similar to the formation of proeutectoid ferrite on the decomposition of austenite.

2.2.5 The partitioning of alloying elements As mentioned previously, the formation of austenite is greatly affected by the addition of alloying elements, which may exert similar effects on the austenitisation reaction as they did on the decomposition reaction since the two transformations have similar characteristics. The role of alloying elements (including carbon) on the austenitisation reaction and the partitioning of these elements between the various phases, has been widely studied.

Judd and Paxton (1968) described a model for the mechanism of the rate of dissolution of carbide in austenite. They proposed that the rate controlling process was carbon diffusion through austenite, that there was local equilibrium at all interfaces and that the diffusion flux of carbon in ferrite

was insignificant. Their experimental results supported this hypothesis and, in addition, found that manganese increased the nucleation incubation period and decreased the nucleation rate of austenite. They suggested that the manganese had either changed the kinetic rate controlling step or altered the boundary conditions for nucleation and that a local increase in the manganese concentration decreased the carbon concentration in austenite and hence lowered the austenite growth rate. The observation that the dissolution of carbides is controlled by carbon diffusion through the growing austenite is supported by Speich and Szirmae (1969). They also found a similar effect for the growth of austenite in pearlite but that carbon played a negligible role on the austenite formation kinetics in a low carbon ferritic steel.

Hillert et al (1971) found that the rate controlling process for the growth of austenite is the diffusion of carbon through the austenite shell around a cementite spheroid. Low alloying element concentrations decrease the overall austenite growth rate by decreasing the carbon diffusion rate in austenite. At a first approximation the growing phase will inherit the alloy content of the phase into which it is growing and that, in general, the chromium and carbon content of the austenite increases with time.

Koch and Eckstein (1978) studied the growth of austenite from ferrite in a 26% Cr, 6% Ni stainless steel. They found that the transformation is controlled by chromium and nickel diffusion, which redistribute simultaneously during the transformation, resulting in an increase in the nickel content of the austenite and the chrome content of the ferrite.

Lenel (1980), investigating an Fe-1,2% Mn-0,1% C alloy, found that the austenitisation reaction between the Ae_1 and Ae_3 temperatures proceeded via two stages. At temperatures below

the no-partition Ae_3, the first stage was carbon diffusion controlled while the second stage was manganese diffusion controlled. Carbon,but not manganese,preferentially partitioned to the austenite during the first stage while both partitioned during the second stage. At temperatures above the no-partition Ae_3, the first stage of austenite growth was controlled by solute drag at the austenite/ferrite interface, while the second stage was manganese diffusion controlled. The austenitisation reaction for a Fe-10% Cr-0,2% C alloy also proceeded via two stages. The first is the nucleation and growth of austenite and is controlled by carbon diffusion through ferrite. Chromium partitioning did not occur. The second stage is the dissolution of alloy carbides in the newly formed austenite and is chromium diffusion controlled.

Wycliffe et al (1981) showed that austenite formation occurred in three stages during the intercritical annealing of an Fe-1% Mn-0,08% C dual phase steel. These stages are: (a) a parabolic growth rate controlled by carbon diffusion with negligible manganese partitioning. This stage was complete within 1-10 seconds. (b) Carbon diffusion fields in austenite impinge and the austenite growth rate is retarded. (c) Manganese partitioning occurs and austenite growth is manganese diffusion controlled. This stage can take up to 100 hours.

Leone and Kerr (1982) studied the growth of austenite from delta ferrite on cooling a high alloy content stainless steeel from the liquid state. They found that the growth of austenite occurred by a diffusion controlled mechanism. Chromium partitioned away from the growing austenite which became enriched in nickel.

2.3 Titanium stabilisation of stainless steel

As discussed in the introduction, Section 1.3.2, stainless steels are susceptible to the precipitation of $Cr_{23}C_6$ type carbides when held for appreciable times at about 700°C. This can be prevented by the addition of small amounts of titanium or columbium which preferentially form carbides, hence leaving chromium in solution. Since 3CR12 is titanium stabilised, the remainder of this discussion will be limited to the stabilisation of stainless steel by titanium alone. This titanium stabilisation effect has long been known and widely studied, e.g. Novak (1977), Demo (1977), Steigerwald et al (1979) and Pickering (1979).

Not only does titanium combine with carbon, it also combines with nitrogen and thus TiC and TiN can form in the same steel. Both have a face centered cubic crystal structure with the carbon and nitrogen occupying octahedral interstices in the lattice. Nitrogen can replace carbon in the carbide and vice versa. The resulting complex constituent is often called titanium carbonitride, Ti(CN). The precipitate which forms depends on the concentration of the three constituents and on the alloy base chemistry. TiN is often bright yellow, while the addition of carbon causes a maize colour to develope. TiC is grey with an undefined shape (Novak, 1977). The titanium can also combine with any sulphur present (Steigerwald et al, 1979) and precipitates in association with the Ti(CN).

For these reasons more than the stoichiometric amount of titanium must be added to the steel to ensure complete stabilisation. A number of formulae which can be used to calculate the amount of titanium needed for stabilisation have been proposed, e.g.

$Ti = 0{,}15 + 3{,}7\ (C + N)$ (Steigerwald et al, 1979)

$Ti = 5\ (C + N)$ (Pickering, 1978)

$Ti \geq 4\ C$ (Lula, 1977)

$Ti = \frac{4C}{f} + 3{,}43\ (N - 0{,}001)$ (Novak, 1977)

where f is a heat treatment factor.

2.4 The morphology and strength of martensite

Characteristics of the martensite reaction (after Christian, 1975) are:

(a) The reaction does not involve diffusion and the composition of the product is necessarily the same as the original phase.
(b) The amount of transformation is virtually independent of time.
(c) The amount of transformation is dependent on temperature, providing other variables such as grain size are constant.
(d) The velocity of the transformation is probably independent of temperature.
(e) There is always a definite relationship between the orientation of the original structure and that of the new phase.

In iron base alloys, there are generally two distinct martensite morphologies. Following the terminology of Krauss and Marder (1971), these two morphologies will be termed lath and plate. Electron microscopy has shown that the basic units in lath martensite are generally aligned parallel to one another in groups called packets. These basic units are called laths and are visible as a fine substructure within the packets. Several packets are formed within a prior austenite grain. Each lath has a high density of tangled dislocations. Krauss and Marder (1971) estimated this dislocation density to be between 0,3 and 0,9 x 10^{12} cm/cm^3. Lath widths have been found to vary from 0,1 to 2,0μm (Apple et al, 1974). The habit plane of the lath martensite is $\{111\}_\gamma$ and it has a body centered cubic crystal structure. Plate martensite has a body centered tetragonal structure and the habit plane is either $\{225\}_\gamma$ or $\{259\}_\gamma$ (Verhoeven, 1975). Unlike laths, adjacent plates do not form parallel to one another. The plates which are the first to form tend to span their parent austenite grains and effectively partition the austenite, thus limiting the size of the plates which subsequently form. This tends to produce a large range of plate sizes. Each plate often has a characteristic midrib.

Thomas (1971) summarised the factors which are thought to be important in controlling the martensite substructure. These are:

(a) Composition: Increasing the total solute content tends to change the morphology from lath to plate, carbon having the strongest effect.

(b) Ms temperature: Decreasing Ms temperature decreases the tendency for lath martensite formation. However, the Ms is linked to the alloy composition.

(c) Strength of martensite: Increasing the strength of martensite decreases the lath tendency, but this property is also dependent on composition. The strength of the parent austenite and its deformation substructure may also influence the morphology.

(d) Austenite stacking fault energy (SFE): A high SFE is supposed to promote laths if the Ms is high. However, increasing the concentration of all solutes promotes plate formation, yet nickel raises, while manganese lowers, the SFE of the austenite.

(e) Cooling rate: A slow cooling rate increases the Ms and hence promotes laths.

(f) Thermal-mechanical: Plastic deformation may cause precipitation in the austenite and hence causes lath martensite to form.

(g) Pressure: At high pressure (i.e. 40kb) plate martensite forms, whereas at atmospheric pressure, lath martensite forms.

The general pattern is that the higher the solute concentration, the greater is the chance of twinned plates forming. Carbon and nitrogen seem to be the most potent elements in promoting the plate morphology. The Ms temperature alone is not the controlling factor.

The strength of martensite can generally be attributed to the interaction of four independent mechanisms:

(a) Solid solution hardening: Strengthening arising from substitutional alloying elements in martensite is quite small. Most of the strength is derived from interstitially dissolved carbon. Speich and Warlimont (1968) found that nickel accounts for approximately one third of the strength of martensite in a carbon free Fe-20% Ni alloy. It is generally found that the strength increases linearly with the square root of the carbon content, e.g. Chilton and Kelly (1968) and Speich and Warlimont (1968). The mechanism for strengthening arises from the elastic interaction between the dislocations and the strains introduced by the individual carbon atoms (Verhoeven, 1975).

(b) Precipitation hardening: Since the martensite is supersaturated with respect to carbon, there is a tendency for the carbon to segregate to interfaces and defects and precipitate as carbides. The segregation occurs in the martensite during the quench and not in the prior austenite. The amount of precipitation is influenced by the Ms temperature and the rate of quench (Chilton and Kelly, 1968).

(c) Structure hardening: This mechanism is only operative in plate martensite. It arises due to the refinement of the prior austenite grain size and hence the martensite plate size (Chilton and Kelly, 1968).

(d) Dislocation hardening: This mechanism is mainly operative in lath martensite. Kehoe and Kelly (1970) found that the strength of lath martensite increased linearly with the square root of the dislocation density. This dislocation density was itself a function of the carbon content. They suggested that the dependence of the strength of lath martensite on the carbon content is indirect and is associated with the carbon dependent dislocation density.

2.5 3CR12

The structure and properties of 3CR12 are under investigation at the Universities of Cape Town, Pretoria and the Witwatersrand and in the laboratories of Middelburg Steel. The various projects include studies of the weldability, corrosion resistance and high temperature mechanical properties of 3CR12.

Protopappas (1983) determined the phase diagram for 3CR12 as a function of nickel content. This is shown in Fig. 2.1. Ball and Hoffman (1981) found partitioning of nickel between the martensite and ferrite of a 1,3% Ni 3CR12 alloy which had been annealed for one hour at 725^{o}C. There was no chromium partitioning. They found a negligible difference in the cell dimensions of the martensite and ferrite, which is in accordance with the low carbon lath structure of the martensite. An EDAX microanalysis indicated that aggregates of sulphides are frequently associated with the titanium carbides.

An investigation into the weldability of 3CR12 was conducted in the Middelburg Steel Laboratories (Martin, 1981). Both 3CR12 and 3CR12 Ni are weldable up to 12mm gauge using AWS 300 series filler electrodes and normal welding procedures. A program to produce a ferritic 3CR12 welding rod has been initiated (Hoffman, 1982). Sondenbergh (1980) found that 3CR12 was susceptible to stress corrosion cracking in $MgCl_2$ solutions above 100^{o}C and that stress accelerated pitting occurred under active conditions in 3,5% NaCl. The corrosion fatigue limit in a 3,5% NaCl solution differed little from that in air. Varying nickel content made no significant difference to the fatigue limit.

Noël (1981) found that as a result of the dual phase nature of the microstructure coupled with its inherent corrosion resistant properties, 3CR12 showed considerable potential as an abrasive-corrosive resistant material for use in mildly corrosive, low stress

abrasive wear environments.

The high temperature mechanical properties of 3CR12 and 3CR12 Ni are being investigated. Brink (1982) showed that between 600^{o} and 1000^{o}C, the ultimate tensile strength of 3CR12 Ni decreases from 891 MPa to 91,6 MPa. The 0,2% proof stress decreases over the same period from 842 MPa to 28,8 MPa.

FIGURE 2.1.

THE IRON–NICKEL PHASE DIAGRAM FOR 3CR12

(from Protopappas, 1983)

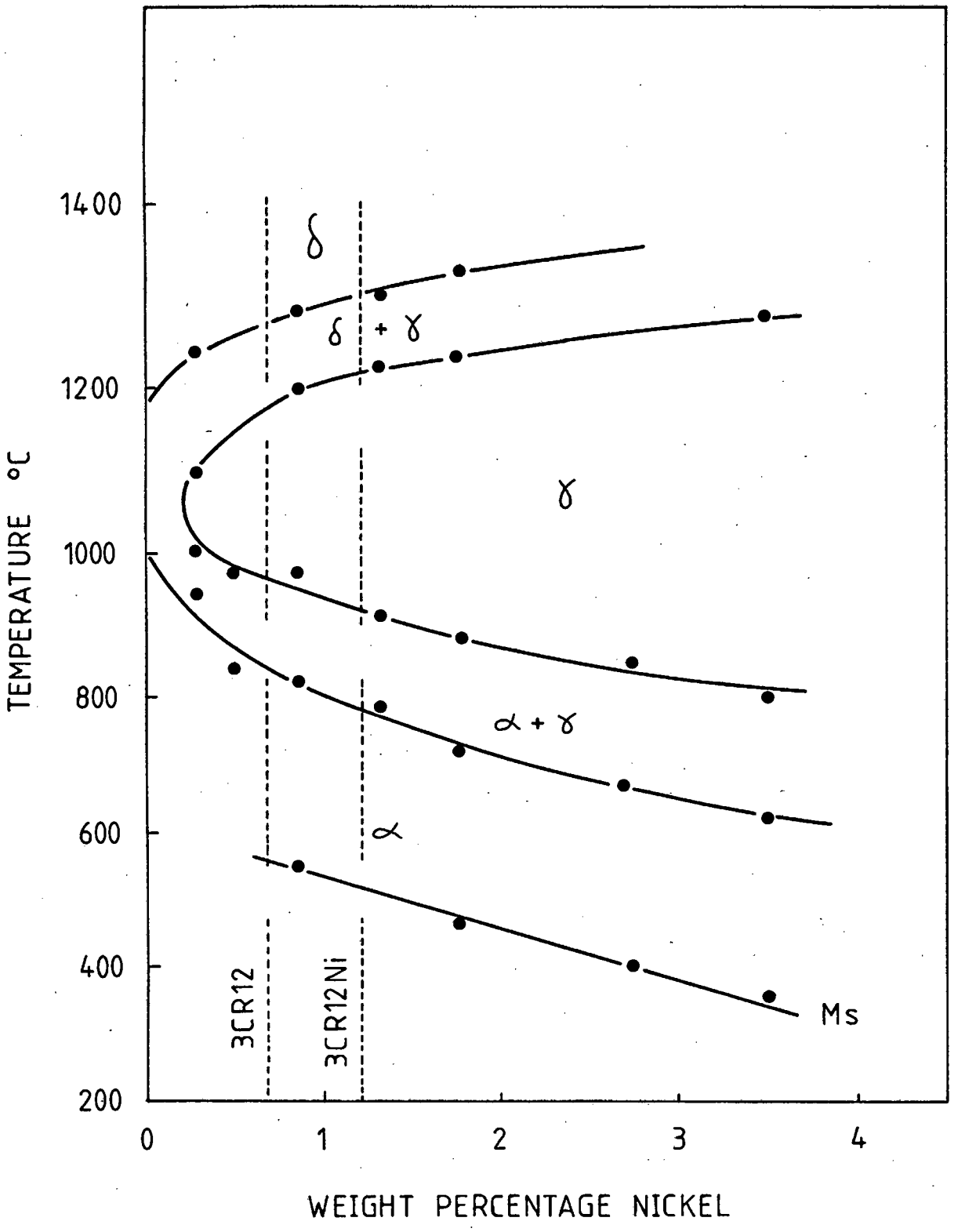

CHAPTER 3 : EXPERIMENTAL METHODS

3.1 Materials used

All the materials were manufactured by Middelburg Steel and Alloys. The 3CR12 and 3CR12 Ni alloys were samples from a normal production run. They were both in the hot rolled condition. The titanium alloys (Ti 1 to 4) were specially prepared in the Middelburg Steel laboratories using an induction melting furnace. The titanium was injected into the melt immediately prior to tapping. The cast ingots were hot rolled and then annealed at 750^{o}C for 33 minutes (80 minutes per inch). The composition of the six steels are given in Table 3.1. These were determined in the laboratories of Middelburg Steel.

TABLE 3.1 : COMPOSITION OF TEST ALLOYS; WT%; BALANCE Fe

	C	S	P	Mn	Si	Ti	Cr	Ni	N_2
3CR12	0,024	0,015	0,020	1,19	0,53	0,31	11,19	0,67	0,011
3CR12Ni	0,027	0,011	0,022	0,90	0,47	0,23	11,71	1,21	0,019
Ti1	0,022	0,015	0,016	1,14	0,37	0,14	11,33	0,62	0,020
Ti2	0,022	0,015	0,016	1,14	0,37	0,20	11,33	0,62	0,020
Ti3	0,022	0,015	0,016	1,14	0,37	0,38	11,33	0,62	0,020
Ti4	0,022	0,015	0,016	1,14	0,37	0,58	11,33	0,62	0,020

3.2 Dilatometry

In the Leitz model UBD dilatometer used, the dilation-temperature curve is generated by the movement of a light spot over photographic paper which is developed after the completion of a test run. The movement of the light spot is controlled by a mirror which is connected to

the specimen by a glass rod. Expansion or contraction of the specimen causes the glass connecting rod to tilt the mirror. This changes its orientation relative to the incident light beam and the position of the light spot on the photographic paper is altered accordingly. A trace of dilation versus temperature is thus obtained.

The dilatometer was used to determine the Ms, Ae_1 and Ae_3 temperatures for all the test alloys. The specimens, dimensioned 4 x 4 x 50mm, were heated to 1000^{o}C at a rate of 5^{o}C/min and then furnace cooled. The transformation temperature was taken as that temperature at which the slope of the dilation curve started to change, since this represents the onset of the phase transformation.

3.3 Heat treatments

3.3.1 Confirmatory tests In order to confirm the transformation temperatures determined dilatometrically, a series of tests were performed on 3CR12 to enable the equilibrium microstructure in each phase regime to be analysed. These tests consisted of annealing specimens, 10 x 10 x 5mm, at 50^{o}C intervals from 800^{o}C to 1100^{o}C for 1 hour, 2 hours and 3 hours; followed by a water quench. A specimen was also annealed at 1000^{o}C for 16 hours and another at 650^{o}C for 12 hours. In addition, a specimen from each of the four titanium alloys was annealed for 1 hour at 100^{o}C above its respective dilatometrically determined Ae_3 temperature.

3.3.2 The austenite decomposition reaction (3CR12) The isothermal transformation reactions were performed in two horizontally opposed tube furnaces which were connected by a porcelain tube. The specimens used were 10 x 10 x 5mm. These were attached by a thin nichrome wire to an AISI 316 stainless steel rod. In

this manner the specimens could be moved quickly and efficiently from one furnace to another and to the quench bath. The reaction sequence consisted of austenitising at 1000°C for 2 hours, followed by an isothermal transformation at 50°C intervals from 650°C to 850°C, for times varying from 1 minute to 16 hours and then water quenching. The hold times were 1 minute, 10 minutes, 100 minutes, 4 hours, 8 hours and 16 hours. Two additional tests were run for 55 minutes at 700°C and 750°C.

3.3.3 The austenite decomposition reaction (3CR12Ni) This transformation was performed using a $BaCl_2$ salt bath. Specimens, 10 x 10 x 15mm, were austenitised in air at 1000°C for 1,5 hours and dropped into a salt bath which was directly under the austenitising furnace. The specimens were reacted at 50°C intervals from 650°C to 800°C for times varying from 6 seconds to 16 hours and then water quenched. The isothermal hold times were 6 seconds, 1 minute, 10 minutes, 100 minutes, 8 hours and 16 hours. Three specimens in the as received condition were annealed at 650°C for 6, 12 and 24 hours and then water quenched.

3.3.4 The austenitisation reaction The same specimen geometry and furnace arrangements as used for the decomposition reaction (3CR12) was used for this transformation. The specimens were fully ferritised at 700°C for 8 hours and then "up-quenched" to temperatures of 810, 860, 915 and 970°C; held for times varying from 5 minutes to 12 hours and immediately water quenched. Heating rates of 970, 915, 860 and 810 °C/min respectively, were obtained. The isothermal hold times were 5 minutes, 15 minutes, 30 minutes, 1 hour, 2 hours, 4 hours, 8 hours and 12 hours. No tests were done at 810°C for 5 minutes or at 915°C and 970°C for 12 hours.

3.4 Metallography

3.4.1 Optical metallography All specimens for optical metallography were mounted in a cold-curing resin, polished in the normal manner and finished with a 0,25μm diamond paste. Two different etchants were used in an attempt to characterise the microstructures. The one was a 10% aqueous oxalic acid solution held at 70°C. The specimens were electroetched with a potential difference of 11 volts for 35 seconds. It was found that warming the solution to 70°C reduced the etching time from approximately 5 minutes to 35 seconds and that the quality of the resulting etch was greatly improved. An aperture diaphram was used to enhance the surface relief of the martensite when viewed in the optical microscope.

The second etch was a colour method recommended for ferritic and martensitic stainless steels by Beraha and Shpigler (1977). The etchant reacts with the specimen and the reaction product is deposited on the surface of the specimen as a thin, interference film causing differential colouration which can be microscopically resolved. The etchant consisted of 3g potassium metabisulfite, 1.5g sulfamic acid and 0.75g ammonium bifluoride in 100ml of distilled water. The etching time was 40 seconds. Immediately after etching, the specimens were rinsed in warm water, washed with alcohol and air dried. Plastic tongs were used at all times.

3.4.2 Transmission electron microscopy Specimens for transmission electron microscopy (TEM) were cut from the same specimens which were used for the optical microscopic investigation of 3CR12. A Metals Research "Microslice" diamond saw was used, and slices ∿0.8mm thick were cut from the same face of the specimen as that imaged optically. When the 3CR12Ni specimens were heat

treated, slices approximately 1mm thick were treated simultaneously by joining the slice and the bulk specimens together with nichrome wire. These slices were then used to produce foils for the TEM.

Discs 3mm in diameter were punched from these slices, mechanically polished to ~0,05mm and then electrochemically polished in a Bainbridge "Unithin" foil thinning unit. The polishing solution was 5% perchloric acid in ethanol. A potential difference of 80V was used which produced a current of approximately 130mA. The polarity was reversed every two seconds. The microscope used was a Joel 200CX operating at 200keV.

3.5 Hardness measurements

The bulk hardness of all specimens was measured using a Vickers pyramid indentor at 30kgf. Each result is the average of five separate indentations.

The microhardness of selected specimens was measured using a microhardness indentor fitted to a Reichart metallurgical microscope. A force of 20 pond was used. Each result is the average of five separate indentations. The hardness is shown as microhardness units (MHU). Microhardness measurements were performed for two reasons; firstly as a method to help distinguish between the martensite and the ferrite and secondly in an attempt to monitor the change in hardness of the martensite phase resulting from the isothermal transformations from ferrite to austenite.

3.6 Volume fraction analysis

The volume fraction of the martensite and ferrite was determined for all specimens which had undergone an austenitisation isothermal transformation and for the 3CR12 specimens used to confirm the trans-

formation temperatures. This was performed by a point counting method as described by Hilliard and Cahn (1961), Hilliard (1968) and Underwood (1970). A 9 x 9 reticule was applied 32 times to each specimen i.e. 2592 points per specimen were counted. This gave a 10% accuracy with a 95% level of confidence. A point counting method was chosen to determine volume fractions because it was the most efficient technique in terms of cost, time and accuracy which was available.

3.7 Chemical microanalysis

A KEVEX micro-X7000 energy dispersive multichannel analytical spectrometer attached to a Cambridge S180 scanning electron microscope was used to detect the amount of free titanium in the four titanium samples. Each specimen was polished to 0,25μm with diamond paste and carbon coated. Since the titanium carbonitrides are significantly harder than the bulk material, they are not polished to the same extent as the bulk and are thus visible in the scanning electron microscope. When the semi-quantitative spot analyses were performed, care was taken to place the beam in an area which was free from these Ti(CN) particles. Each specimen was analysed five times using an accelerating voltage of 15keV and an interaction area of approximately 10μm.

A Cambridge Microscan 5 electronprobe microanalyser was used to perform a standardless analysis on 3CR12 in order to determine if and when nickel or manganese had partitioned during the austenitisation isothermal transformations. Specimens for analysis, which had been austenitised at 860^{o}C for 15 and 30 minutes, were mounted in bakelite resin, polished and then etched in oxalic acid. The probe was placed over adjacent ferrite and martensite grains and each specimen was analysed twice. The results obtained were the number of x-ray counts recorded in 10 seconds.

CHAPTER 4 : RESULTS

4.1 The transformation temperatures of 3CR12

The dilatometrically determined Ae_1 and Ae_3 temperatures were 792°C and 856°C, respectively. The Ms temperature, on furnace cooling, was 456°C. The trace is shown in Fig. 4.1. Specimens annealed above 856°C should, therefore, be fully austenitic. However, metallography of the specimens annealed at 900°C to 1100°C showed that 3CR12 never became fully austenitic. The microstructures of the specimens treated for 1, 2 and 3 hours at each test temperature showed no significant change, while after 16 hours at 1000°C, the ferrite grains, though fewer in number, had grown significantly. Micrographs of the specimens annealed for two hours are shown in Fig. 4.2. A TEM micrograph of the specimen annealed at 1000°C for 2 hours is shown in Fig. 4.3. A ferrite grain, of the same basic shape as those imaged optically, is clearly visible in a lath martensitic matrix. The hardness of the matrix in the 16 hour specimen was 250MHU and of the ferrite was 176MHU. These results indicate that phase equilibrium had been achieved after 1 hour and that annealing for longer times promoted grain growth.

It is evident from these micrographs and hardness measurements that ferrite is present in all these structures. The volume fraction of the ferrite at 1000° was 0,08, increased to 0,13 at 1050°C and to 0,40 at 1100°C.

FIGURE 4.1.

DILATOMETRIC TRACE OF 3CR12 SHOWING PHASE TRANSFORMATION TEMPERATURES

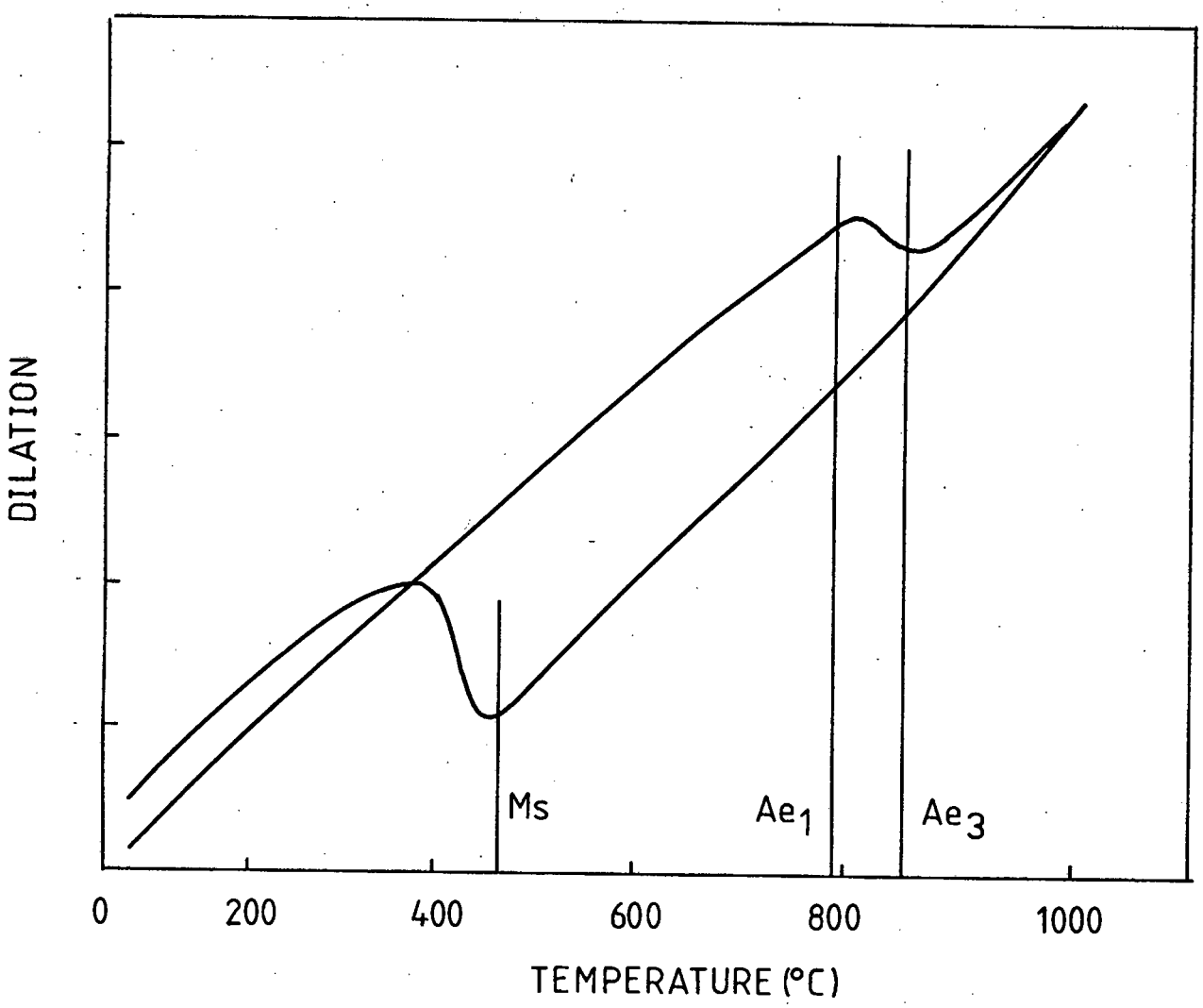

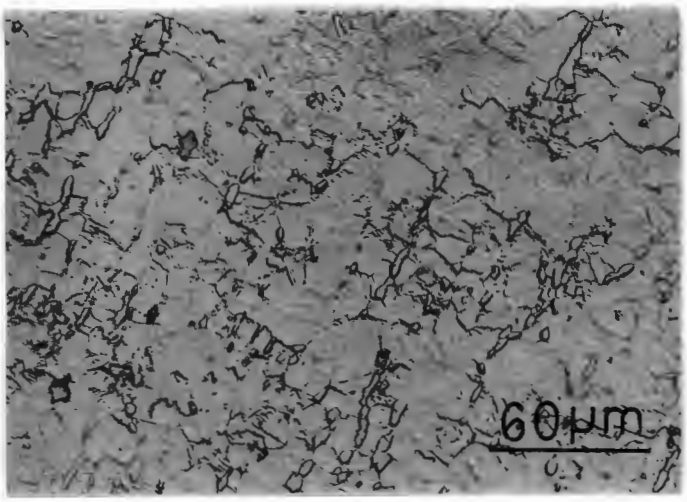

900°C

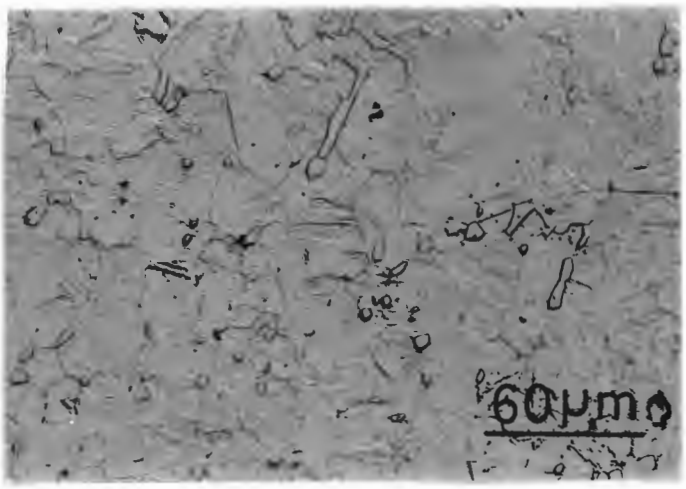

950°C

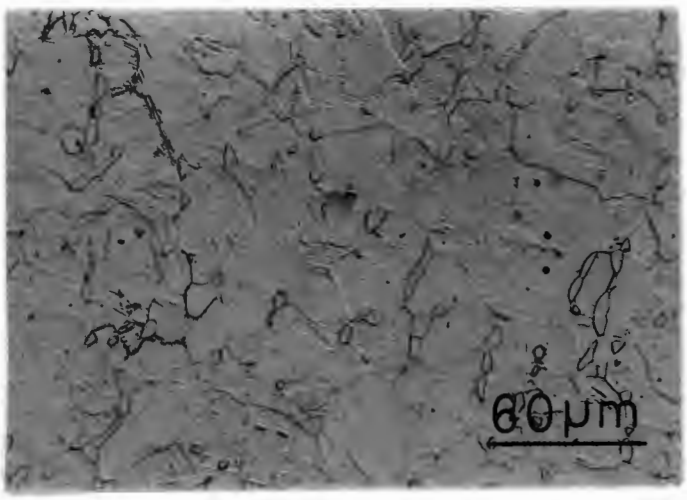

1000°C

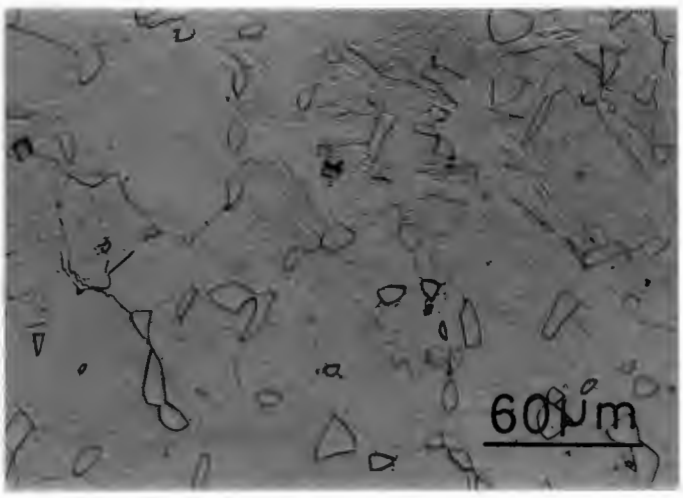

1050°C

Figure 4.2 3CR12 after 2 hour anneal showing small ferrite grains in austenite (now martensite) matrix.

Figure 4.3 TEM micrograph of 3CR12; 1000°C, 2 hours showing a ferrite grain in a lath martensite matrix.

4.2 The austenite decomposition reaction (3CR12)

The microstructure of the starting structure (1000°C for 2 hours) for the austenite decomposition reaction was discussed in the previous section. The decomposition reaction showed three distinct regimes.

At 650°C and 700°C "new" ferrite nucleated, grew at the expense of austenite and the structure became fully ferritic after 16 hours at 650°C and after 8 hours at 700°C. The new ferrite was sympathetically nucleated i.e. it nucleated at existing ferrite/austenite boundaries. This is clearly evident in Fig. 4.4 which shows a micrograph of a specimen which had been isothermally transformed at 650°C for 4 hours. The austenite (now martensite) is blue/green, the old ferrite yellow and the sympathetically nucleated new ferrite is mauve-brown. The TEM analysis confirmed that the new ferrite was sympathetically nucleated; typical examples are shown in Fig. 4.5. Fig. 4.5 (a) shows a ferrite grain in a lath martensite matrix. This grain has a similar morphology to those which were present in the starting structure. There now appears, however, to be a subgrain boundary in the ferrite. This boundary, which consists of tangles of dislocations around precipitates, constituted the original ferrite boundary and the structure around this is the new ferrite which nucleated and grew during the hold time at 650°C. The ferrite in Fig. 4.5 (b) consists of four grains. The triangularly shaped internal grain was the original ferrite around which the new ferrite had nucleated. There appear to be three new grains, with grain boundaries radiating from the corners of the triangle. The fully ferritic structure is shown in Fig. 4.6. The original ferrite grains are still visible, although their boundaries have become diffuse and indistinct.

At 750°C no new ferrite nucleated. Optical metallography (Fig. 4.7) has shown that the ferrite grains appear to have become slightly enlarged and the grain boundaries have become undefined compared to the distinct boundaries of the starting structure. TEM (Fig. 4.8) showed that the ferrite boundaries are highly convoluted and irregular. No subgrain

boundary is visible. These convolutions could be the cause of the fuzziness of the ferrite imaged optically.

At 800°C and 850°C, no change was observed in the microstructure at any time for which the specimens were tested.

The bulk hardness of the 650°C and 700°C transformation series dropped from approximately 270VPN (of martensite, which was austenite in the starting structure) to approximately 150VPN (the fully ferritic structure). The 700°C series decreased over a shorter time period and to a marginally lower value than the 650°C series. The hardness of the 750°C series dropped to approximately 225VPN, while the 800°C and 850°C series showed no significant change. The hardness measurements are presented in Table 4.1 and illustrated in Fig. 4.9.

Two distinct carbide morphologies have been discerned. These are interphase precipitation and random precipitation on dislocations. The two appear to be mutually exclusive, that is, if the one mode of carbide precipitation has occurred in a ferrite grain, then the other has not. Both types of precipitation have occurred in specimens transformed at 650°C and 700°C, whereas no significant carbide deposition has occurred in specimens transformed at 750°C. Fig. 4.10 (a) is a magnified view of a portion of the ferrite shown in Fig. 4.5 (b). Interphase precipitation has occurred in the right hand grain, whereas precipitation on dislocations has occurred in the left hand grain. Fig. 4.10 (b) is a TEM micrograph of a specimen isothermally transformed at 700°C for 100 minutes. Interphase precipitation has occurred in the sympathetically nucleated ferrite grain which grew into the austenite (now martensite) matrix.

On the basis of the above results, a TTT diagram has been drawn (Fig. 4.11) which shows the beginning and the end of the transformation to ferrite, and the three phase regions: austenite plus 8% ferrite, austenite plus ferrite and ferrite plus associated carbides. The curves demarcating the phase fields are inferred and are not intended to illustrate the exact transition points.

TABLE 4.1 : 3CR12: HARDNESS VALUES (VPN) FOR THE ISOTHERMAL DECOMPOSITION OF AUSTENITE

TIME	650°C	700°C	750°C	800°C	850°C
1 min	275	258	270	264	287
10 min	278	254	247	286	276
55 min	-	250	232	-	-
100 min	275	246	230	278	242
4 hr	249	157	217	298	242
8 hr	194	147	215	270	249
16 hr	158	138	213	269	256

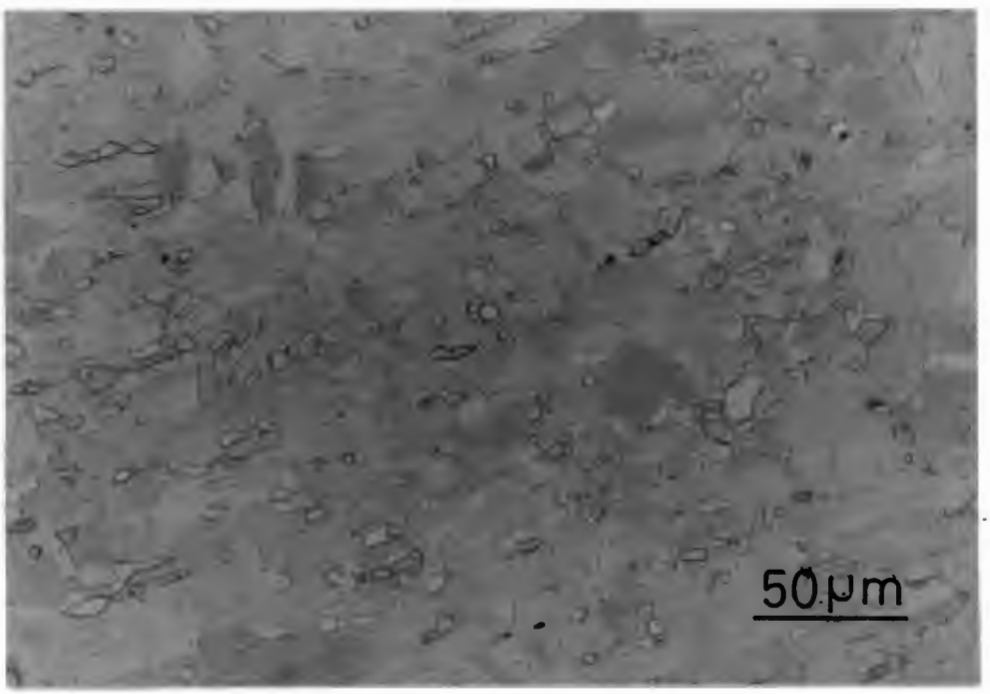

Figure 4.4 Sympathetic nucleation of ferrite in 3CR12 isothermally transformed at 650°C for 4 hours. The austenite (now martensite) is blue/green, the old ferrite yellow and the new ferrite is mauve/brown.

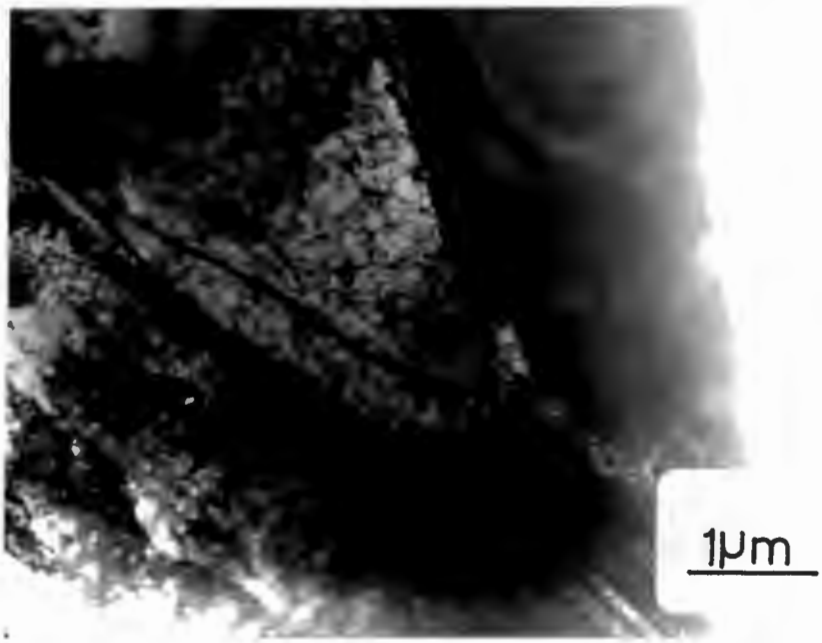

(a) 650°C, 8 hours

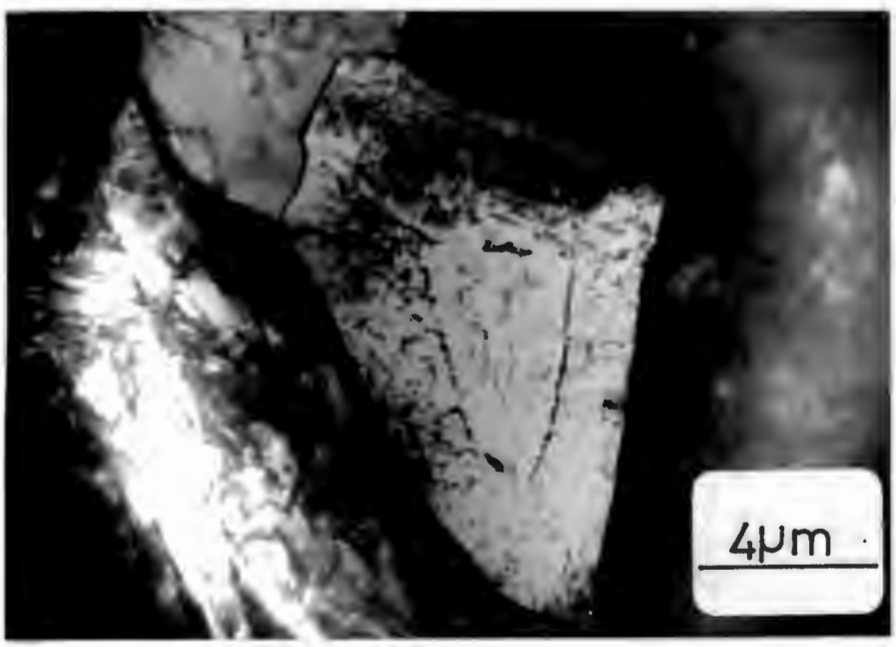

(b) 700°C, 100 minute

Figure 4.5 TEM micrographs of 3CR12 showing sympathetic nucleation of ferrite during isothermal decomposition of austenite.

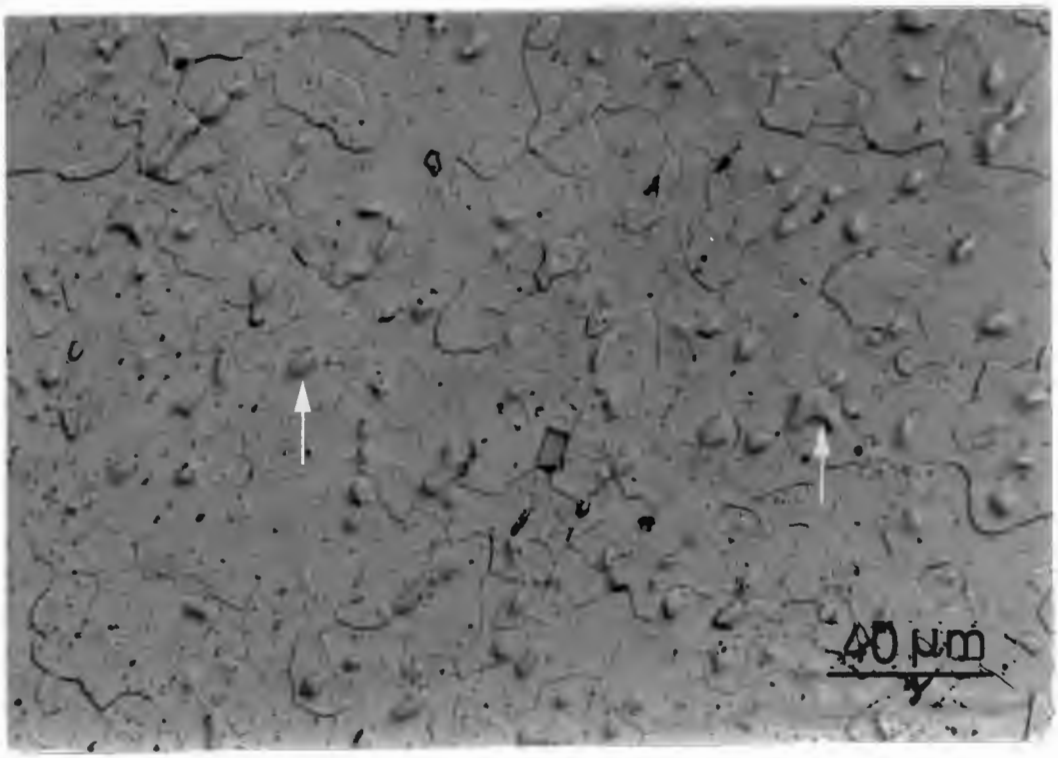

Figure 4.6 Fully ferritic 3CR12 structure after isothermal transformation at 700°C for 8 hours. The original ferrite grains are indicated.

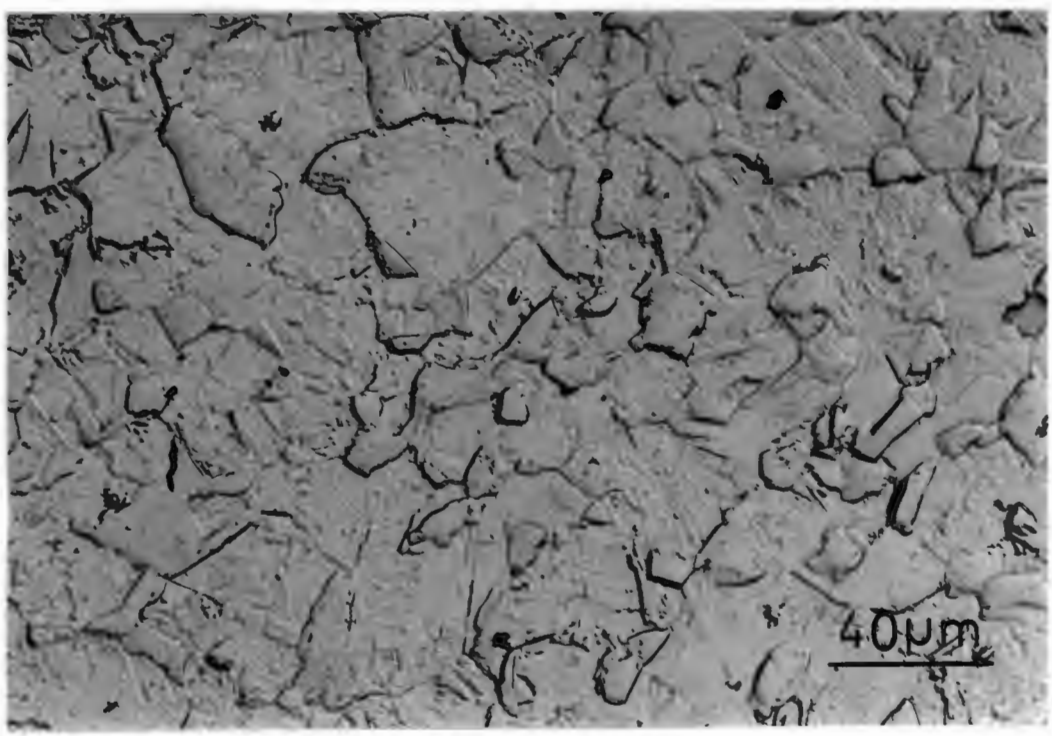

Figure 4.7 Irregular ferrite grains in austenite (now martensite) matrix after isothermal transformation at 750°C for 8 hours.

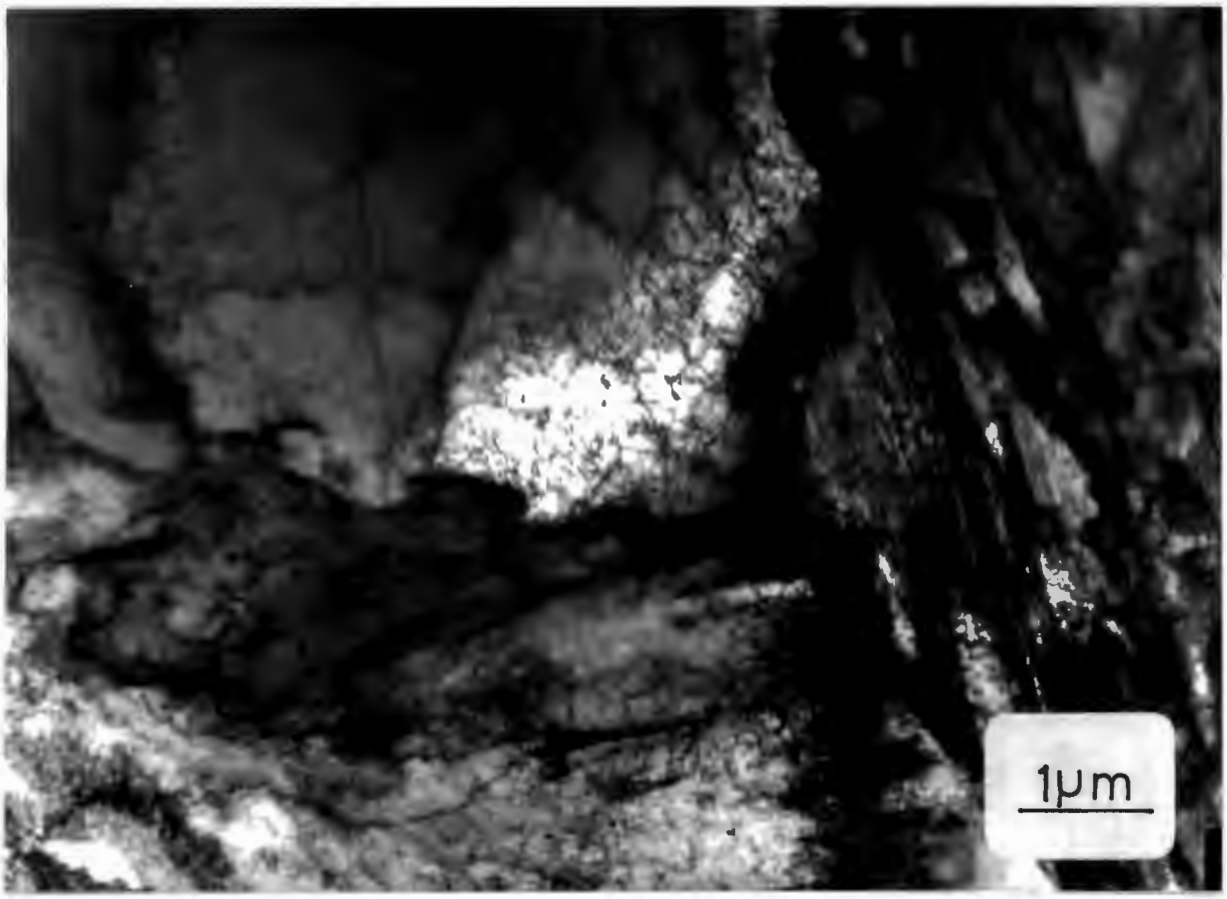

Figure 4.8 Convoluted ferrite grain in austenite (now martensite) matrix after isothermal transformation of 3CR12 at 750°C for 8 hours.

FIGURE 4.9.

3CR12: HARDNESS vs. TIME FOR ISOTHERMAL DECOMPOSITION OF AUSTENITE

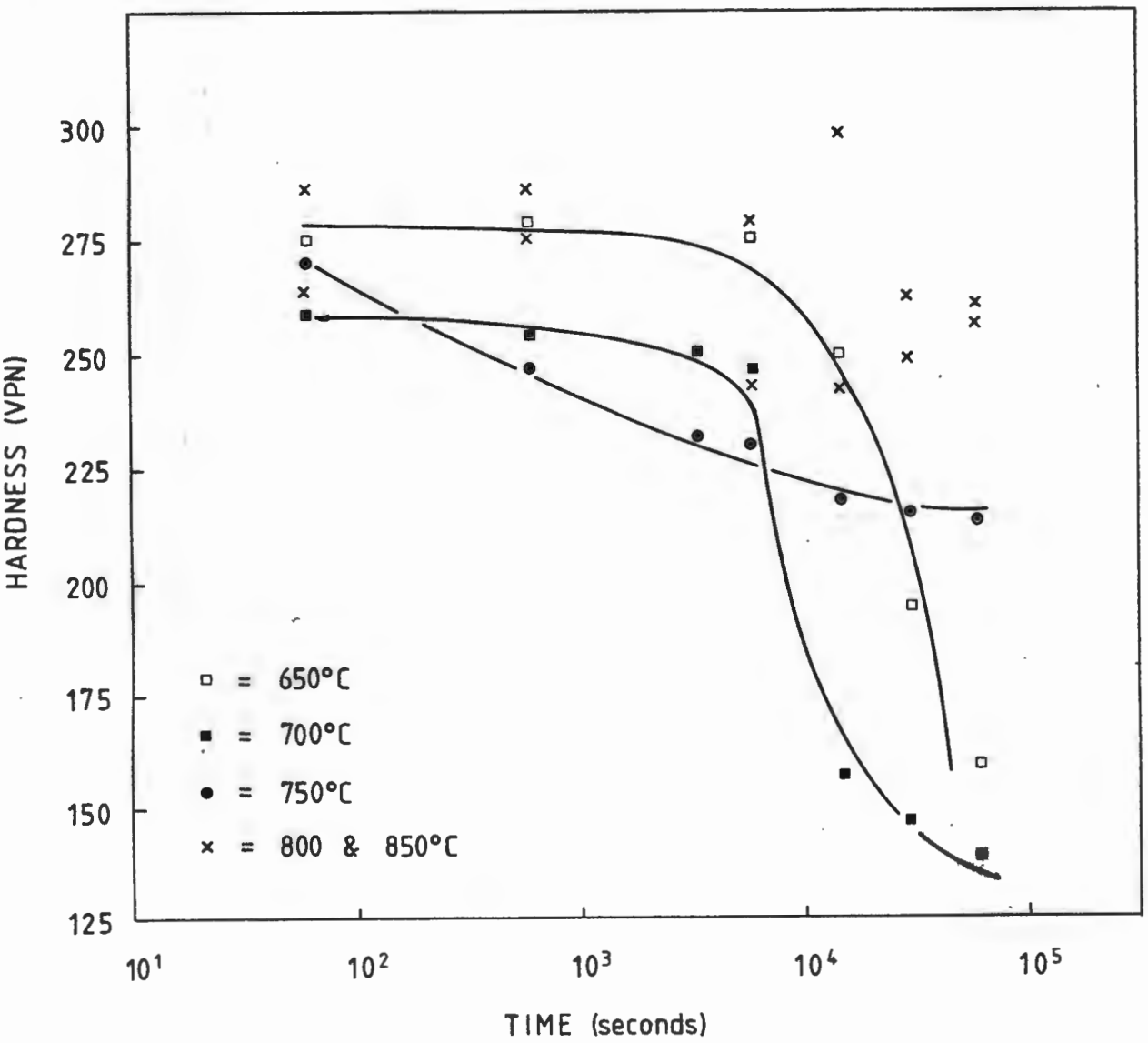

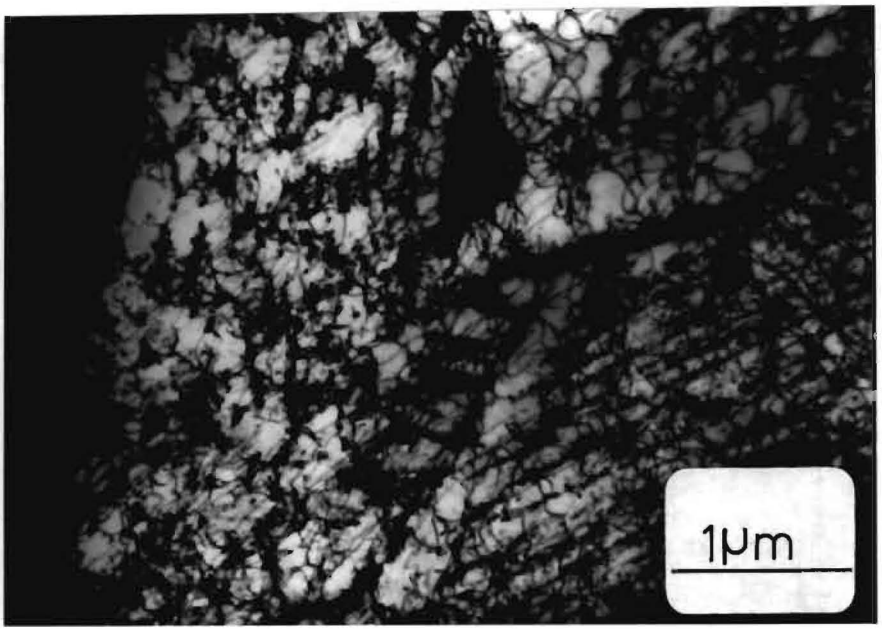

(a)

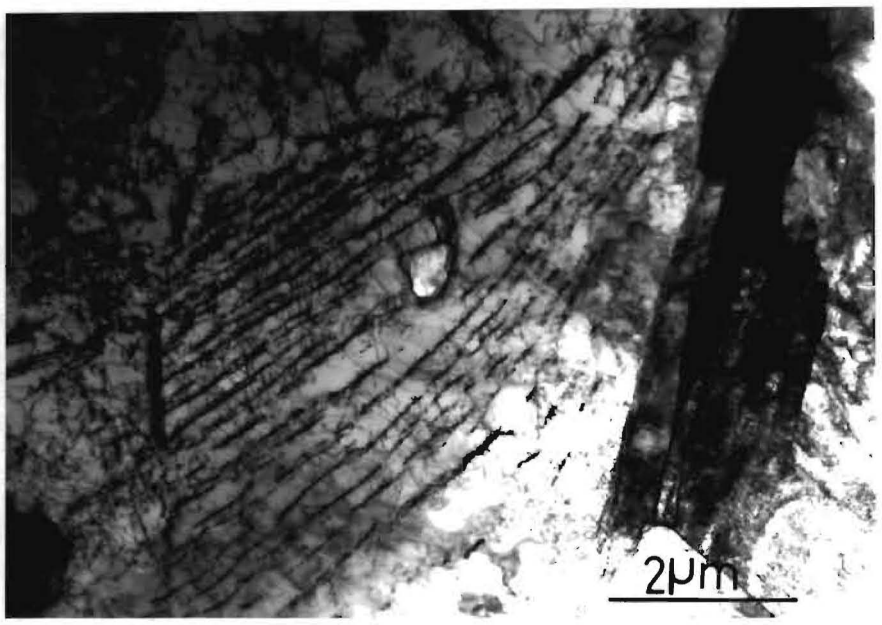

(b)

Figure 4.10 Precipitation of carbides in ferrite on isothermal transformation of 3CR12 at 700°C for 100 minutes.

(a) Magnified view of portion of Fig. 4.5 (b) showing interphase precipitation in the right hand grain and precipitation on dislocations in the left hand grain.

(b) Sympathetic nucleation of ferrite showing interphase precipitation.

FIGURE 4.11.

3CR12: ISOTHERMAL TRANSFORMATION DIAGRAM:

DECOMPOSITION OF AUSTENITE

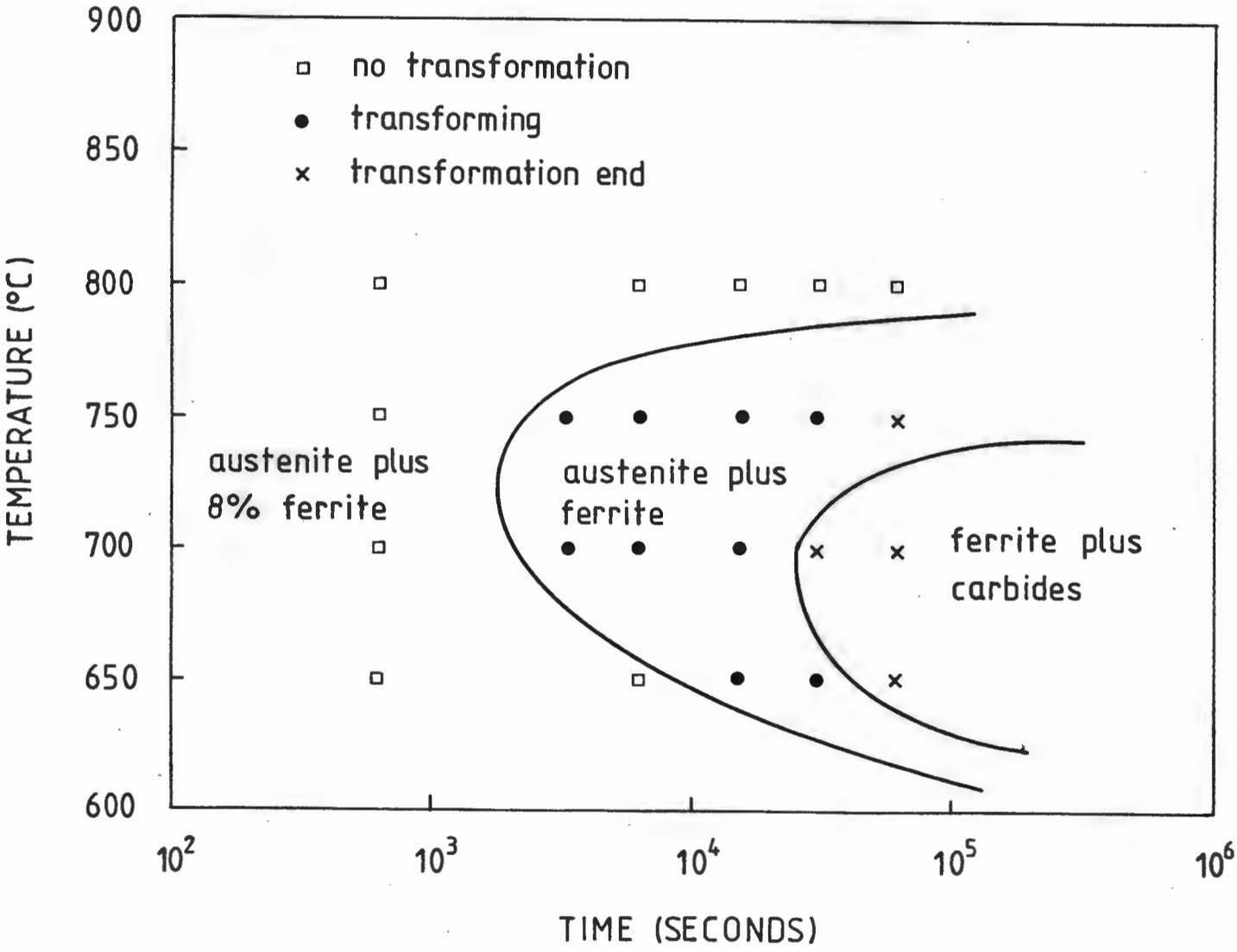

4.3 The austenitisation reaction

The starting structure for the austenitisation reactions consisted of equiaxed ferrite grains with an associated dispersion of fine carbides on dislocations and along the grain boundaries. At 810°C and 860°C i.e. at temperatures between the Ae_1 and Ae_3 and marginally above the Ae_3, respectively, the austenitisation reaction proceeded extremely slowly. At 810°C, the reaction was only 10% complete after 1 hour and took 12 hours to approach equilibrium. At 915°C the reaction was complete after 30 minutes and at 970°C after 5 minutes. The austenite volume fractions for the isothermal transformations are presented in Table 4.2 and illustrated in Fig. 4.12. A TTT curve was constructed from these results (Fig. 4.13). "C" shape kinetics did not occur; the reaction rate increased with increasing temperature. At no combination of time and temperature did the alloy become fully austenitic. This was expected in terms of the results presented in the previous sections.

The sluggishness of the reaction allowed the different nucleation morphologies to be studied. Optical microscopy (Fig. 4.14) showed that austenite (now martensite) initially nucleated at ferrite grain boundaries. After a limited growth period, intragranular idiomorphs and plates were observed, while sideplates had grown from the original grain boundary allotriomorphs. Optical microscopy, however, could not determine whether these idiomorphs and plates had indeed nucleated intragranularly or had merely grown from an allotriomorph which had nucleated at a grain boundary below the plane of the imaged grain and subsequently grown into this grain. To resolve this dilemma, selected specimens were examined using TEM. No evidence was found forany intragranular nucleation. Austenite had nucleated at grain boundaries and triple points in the ferrite matrix. Fig. 4.15 (a) shows an austenite (now martensite) grain which had nucleated at a triple point and grown along the ferrite/ferrite grain boundary. The increase in dislocation density immediately adjacent to the martensite grain is due to the

volume change which occurred during the transformation from austenite on quenching. Fig. 4.15 (b) shows a later stage of austenite growth. Austenite (now martensite) has nucleated at a ferrite/ferrite grain boundary and grown into both adjacent grains. A secondary sideplate is visible. An extensive search was conducted in an attempt to detect retained austenite. However, no such evidence was found and it was not possible, therefore, to determine the orientation relationships between the austenite and the ferrite matrix.

The results of the electron microprobe investigation are presented in Table 4.3. It appears that nickel and manganese did not initially partition between the austenite and the ferrite but that a limited period of austenite growth was required before partitioning occurred. The values presented are not intended as accurate measurements of partitioning but are merely indicative of a general phenomenon. Microhardness measurements were conducted on specimens treated for various times and temperatures so that a wide range of martensite volume fractions could be tested. Fig. 4.16 shows a plot of the volume fraction of martensite versus the hardness of the martensite. Although the inaccuracies are large it nevertheless shows a definite trend: the more martensite in the specimen the harder this martensite becomes. The errors could have arisen from a number of sources e.g. differential work hardening of the surface due to polishing, vibrations during testing or a nonplanar specimen surface. For the purposes of the present investigation, these errors are not significant since absolute values are not derived from the diagram and are not necessary in the analysis of the underlying trend. The bulk hardness values of the austenitisation specimens are presented in Table 4.4.

TABLE 4.2 : VOLUME AUSTENITE (%) FOR AUSTENITISATION TEST SPECIMENS

TIME	810°C	860°C	915°C	970°C
5 min	-	2	85	92
15 min	-	31	85	95
30 min	-	72	88	95
1 hr	10	77	90	95
2 hr	8	79	92	96
4 hr	30	82	92	96
8 hr	43	85	93	96
12 hr	62	85	-	-

TABLE 4.3 : MICROANALYSIS OF AUSTENITISATION TEST SPECIMENS, 800°C

(NUMBER OF X-RAY COUNTS IN 10 SECONDS)

TIME (mins)	NICKEL			MANGANESE		
	γ	α	γ / α	γ	α	γ/α
15	4341	4310	1,01	9093	8938	1,02
30	4662	3762	1,24	8958	8059	1,11

TABLE 4.4 : HARDNESS (VPN) OF AUSTENITISATION TEST SPECIMENS

TIME	810°C	860°C	915°C	970°C
5 min	-	151	256	281
15 min	142	200	246	282
30 min	146	220	258	282
1 hr	156	233	269	277
2 hr	154	230	261	282
4 hr	183	239	261	278
8 hr	195	238	264	270
12 hr	201	234	-	-

FIG. 4.12. VOLUME FRACTION AUSTENITE vs. TIME FOR ISOTHERMAL TEST TEMPERATURES

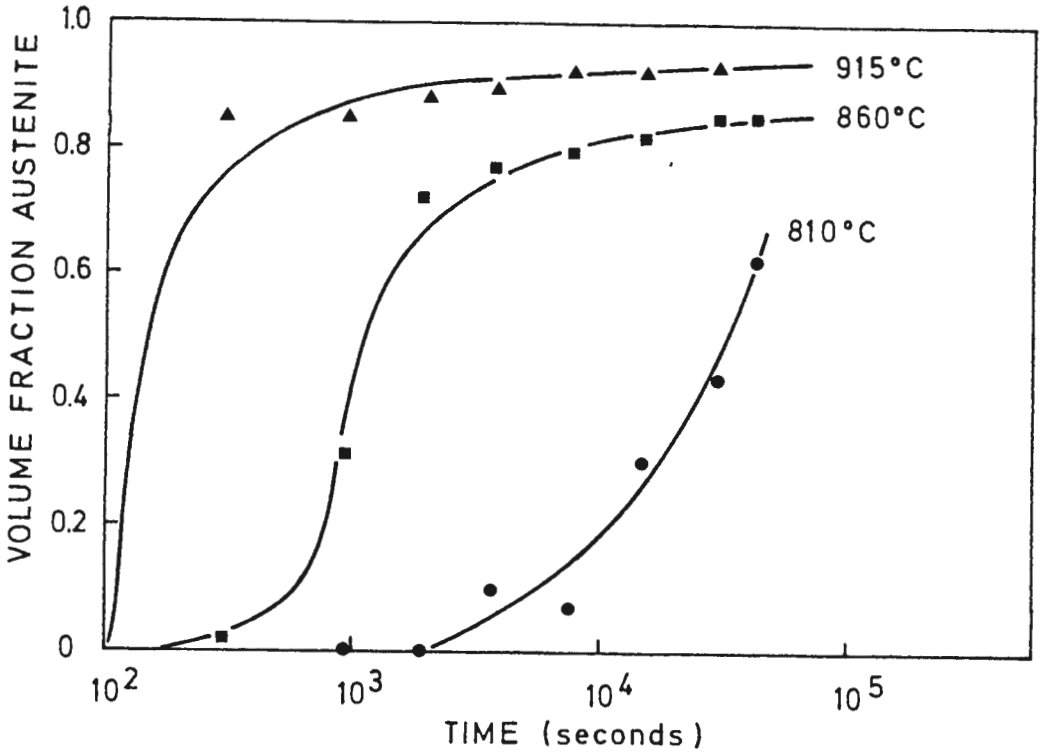

FIG. 4.13. AUSTENITISATION ISOTHERMAL TRANSFORMATION DIAGRAM

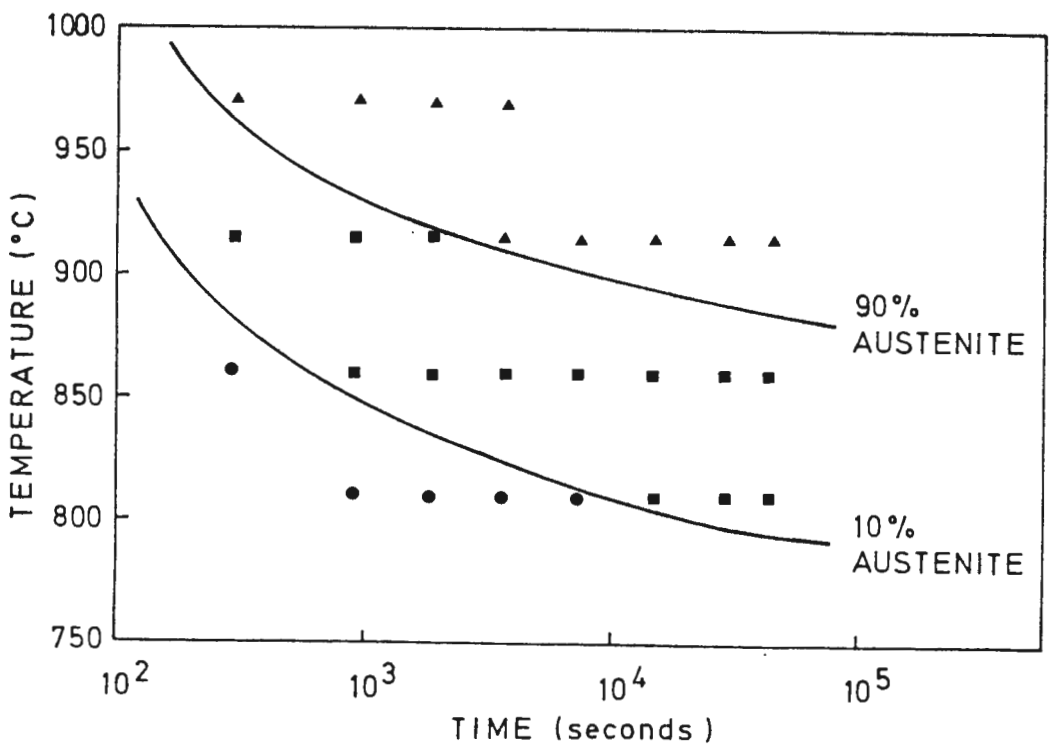

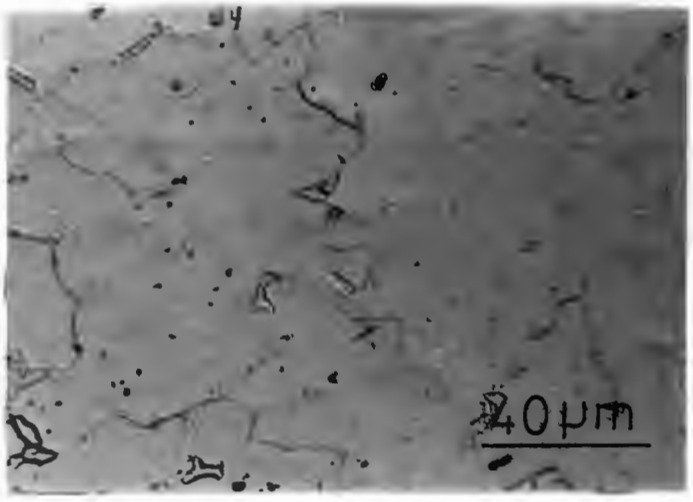

5 minutes

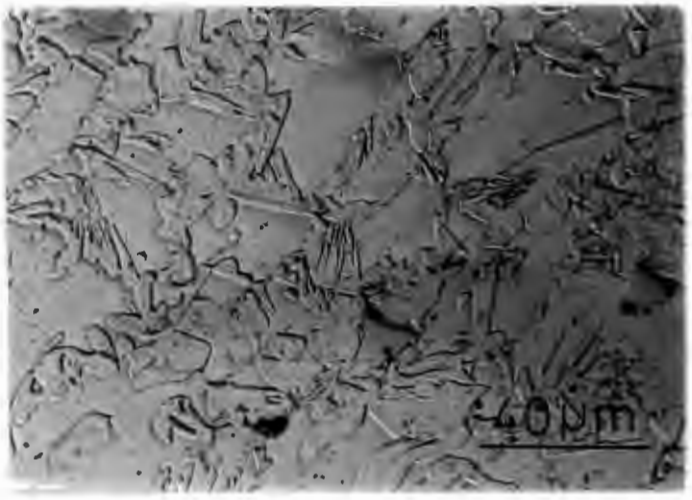

15 minutes

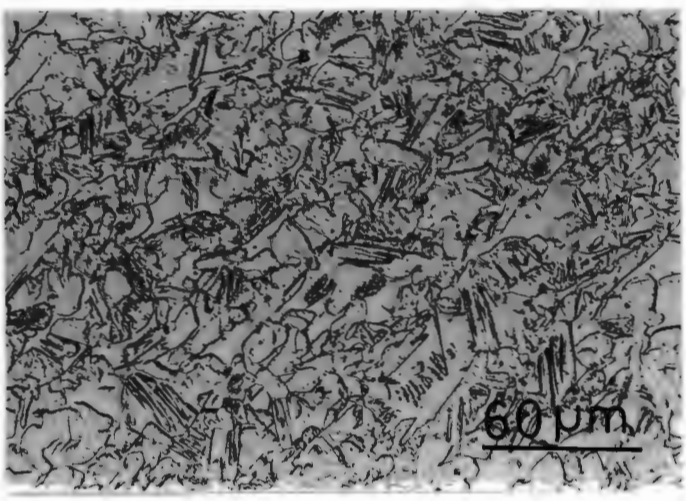

30 minutes

Figure 4.14 Isothermal transformation of ferrite, 860°C.

(a)

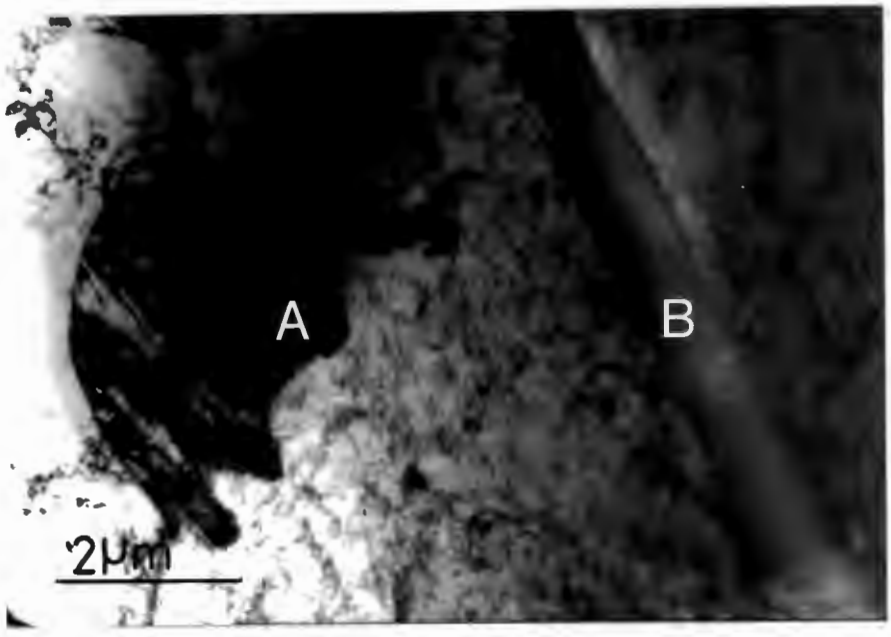

(b)

Figure 4.15 Isothermal transformation of ferrite at 860°C showing austenite (now martensite) growing in a ferritic matrix.

(a) 5 minutes. Austenite (now martensite) grain boundary allotriomorph.

(b) 15 minutes. Grain boundary allotriomorph (A) and secondary side-plate (B) of austenite (now martensite) in ferrite matrix.

FIGURE 4.16.

HARDNESS OF MARTENSITE vs. VOLUME FRACTION MARTENSITE FOR AUSTENITISATION ISOTHERMAL TRANSFORMATIONS

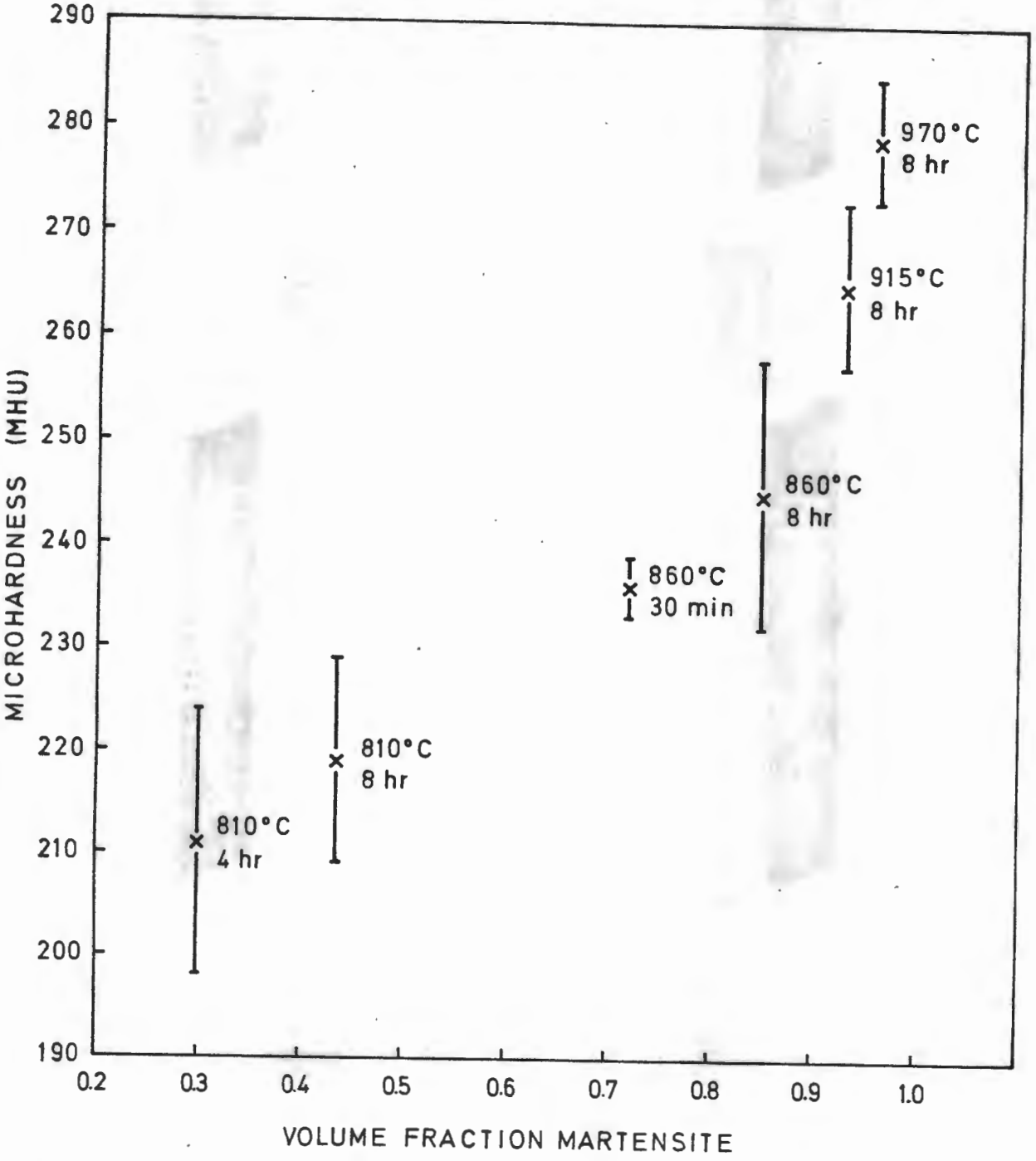

4.4 The austenite decomposition reaction (3CR12Ni)

The dilatometrically determined Ms, Ae_1 and Ae_3 temperatures were 389°C, 745°C and 842°C, respectively. The microstructure of the starting structure (1000°C for 1½ hours) for the austenite decomposition reaction consisted of small ferrite grains in an austenite matrix. The ferrite grains were elongated into stringers which were roughly parallel to each other. This morphology arose from the as-received, hot rolled condition (Fig. 4.17). Optical micrographs of the decomposition starting structure are shown in Fig. 4.18. Colour metallography shows the austenite (now martensite) matrix in two colours (blue and brown), while some grains appear to be a complex mixture; neither blue nor brown. The ferrite grains are small, elongated and pale yellow/green. The hardness of the dark blue martensite grains was 273MHU and the dark brown martensite grains was 239MHU. The bulk hardness value was 329VPN. The different matrix colours and hardness values could possibly have arisen from martensite packets lying at slightly different orientations to the surface and hence having different etch and hardness characteristics. A TEM micrograph of the same structure is shown in Fig. 4.19. The martensite laths vary in width from approximately 0,1 to 1,0µm and have an extremely high dislocation density. Packets of laths with different orientations lie within a prior austenite grain. Each packet consists of a number of different laths lying parallel to each other.

Metallography, both optical and TEM, showed that no significant change had occurred in the alloy at any time or temperature for which it was isothermally transformed in order to study the "decomposition reaction". The bulk hardness measurements (Table 4.5) of these specimens did not show any significant change during the isothermal transformations. The hardness should have decreased if ferrite had grown out of the austenite matrix. The hardness measurements therefore confirmed the microstructural analysis.

Specimens in the as-received condition, which were then annealed at 650^{o}C for 6 and 12 hours, showed limited ferrite growth. However, a fully ferritic structure was realised in a specimen annealed under the same conditions for 24 hours. The hardness of the specimens annealed for 6, 12 and 24 hours were 252, 215 and 177 VPN, respectively.

TABLE 4.5 : 3CR12Ni : HARDNESS VALUES (VPN) FOR THE ISOTHERMAL DECOMPOSITION OF AUSTENITE

TIME	650°C	700°C	750°C	800°C
6 sec	317	305	314	308
1 min	302	321	311	311
10 min	305	304	309	304
100 min	312	311	307	315
8 hr	308	309	295	311
16 hr	297	312	315	309

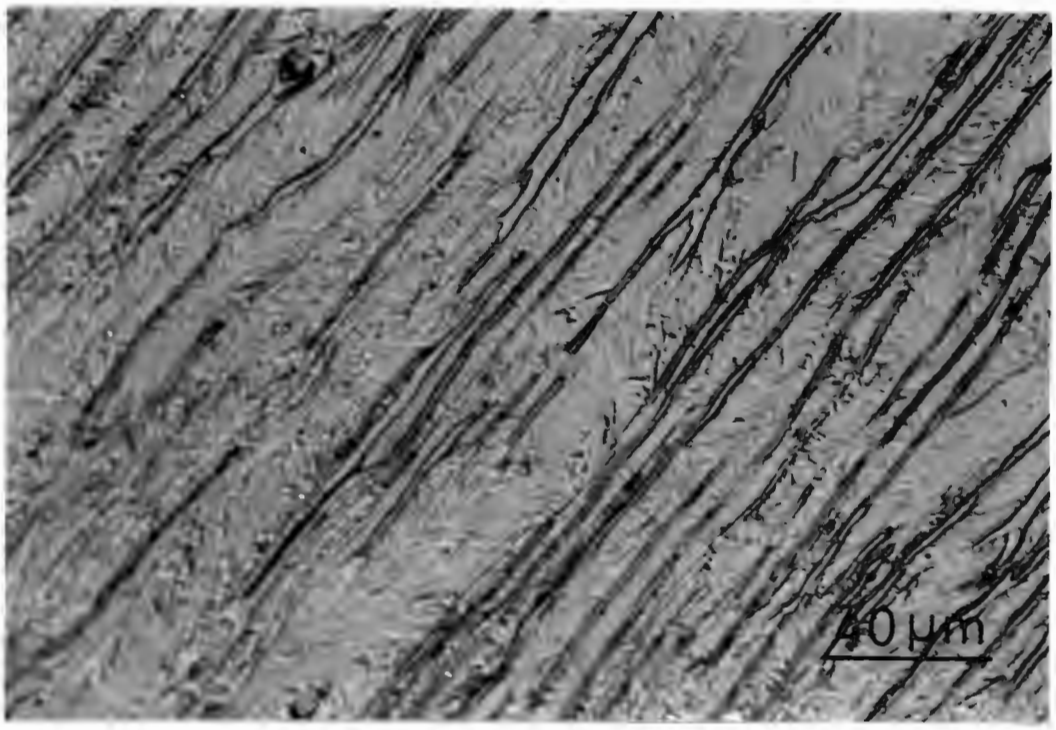

Figure 4.17 3CR12Ni, as-received condition showing ferrite stringers in a martensitic matrix.

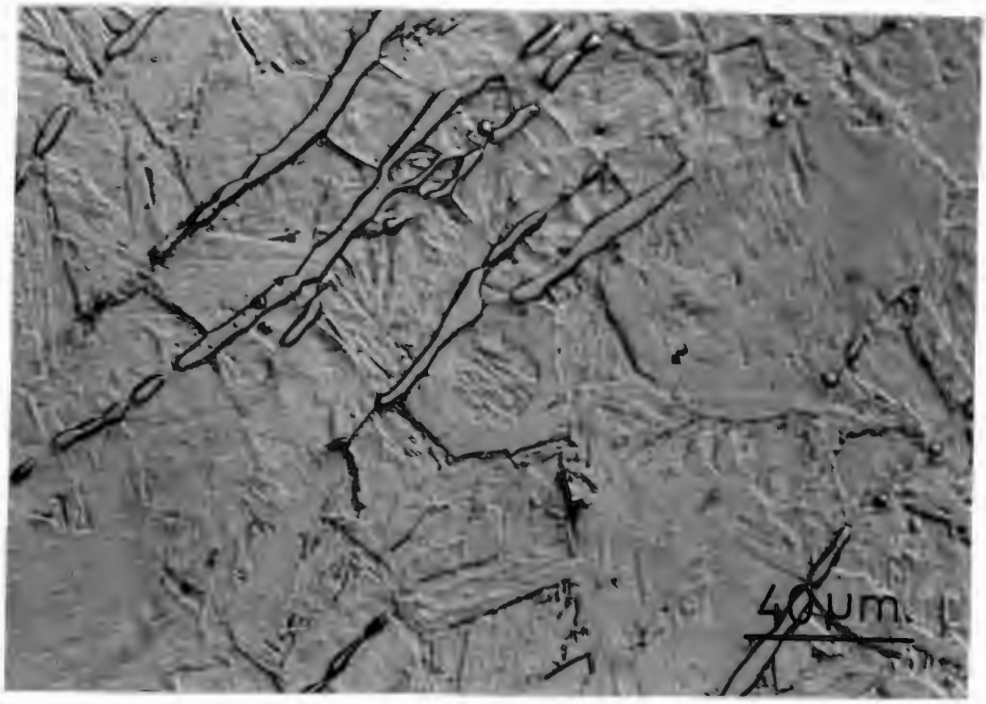

(a)

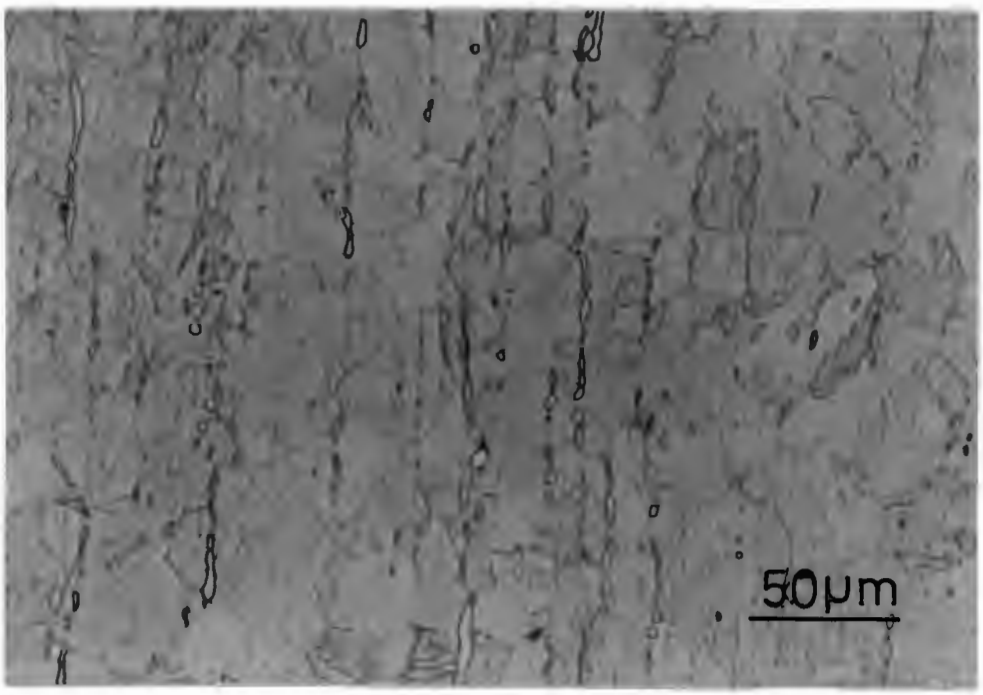

(b)

Figure 4.18 3CR12Ni after 1½ hours anneal at 1000°C.

(a) Oxalic acid etch.

(b) Colour etch; the martensite appears blue and brown and the ferrite yellow/green.

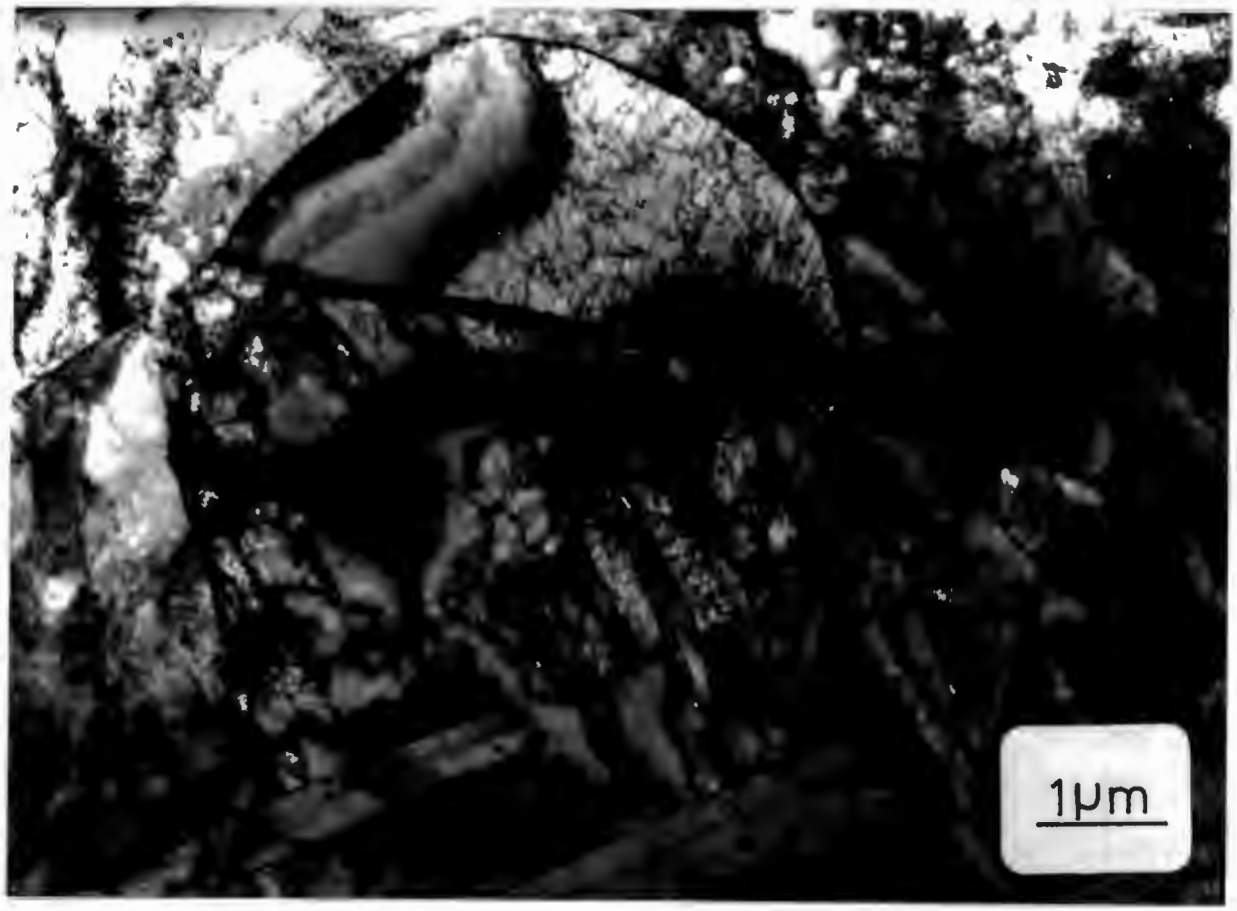

Figure 4.19 3CR12Ni after 1½ hour anneal at 1000°C showing a ferrite grain in a lath martensite matrix.

4.5 The titanium effect

The Ms, Ae_1 and Ae_3 temperatures, calculated from dilatometry, are presented in Table 4.6 and illustrated graphically in Fig. 4.20. All three transformation temperatures increased continuously with increasing titanium content. The increase in the Ms temperature seems to be approaching a limiting value, although this may be due to a decrease in the rate of increase and that there is not necessarily a maximum value. None of the four alloys became fully austenitic above their Ae_3 temperatures, although for specimen 1 annealed at 940°C, the ferrite volume fraction was 0,01. The microstructures of the four alloys in the as-received condition, i.e. annealed at 750°C, with their respective hardness values, are shown in Fig. 4.21.

The results of the microanalysis of the four specimens are presented in Table 4.7. Free titanium was shown to be present in all four specimens. Since the analyses did not include all the alloying elements present in the steels, that the technique is such that the weight percentage of all the elements together must equal one hundred, and that it was a standardless analysis, the results do not necessarily represent the exact amount of titanium present. One of the five tests on specimen 1 did record a zero titanium content. The results therefore show that free titanium is indeed present in all the specimens and that this free titanium content increases with an increasing amount of bulk titanium.

TABLE 4.6 : VARIATION IN TRANSFORMATION TEMPERATURES WITH TITANIUM CONTENT, ^{o}C

Sample	Ms	Ae_1	Ae_3
1	425	777	839
2	443	800	861
3	556	842	893
4	577	864	934

TABLE 4.7 : KEVEX MICROANALYSIS OF TITANIUM SPECIMENS, WT%

Sample	Ti	Cr	Mn	Ni
1	0,05	11,08	2,14	0,66
2	0,06	11,37	2,19	0,84
3	0,13	10,95	2,17	0,71
4	0,28	10,96	2,18	0,70

FIGURE 4.20.

VARIATION IN TRANSFORMATION TEMPERATURES WITH TITANIUM CONTENT

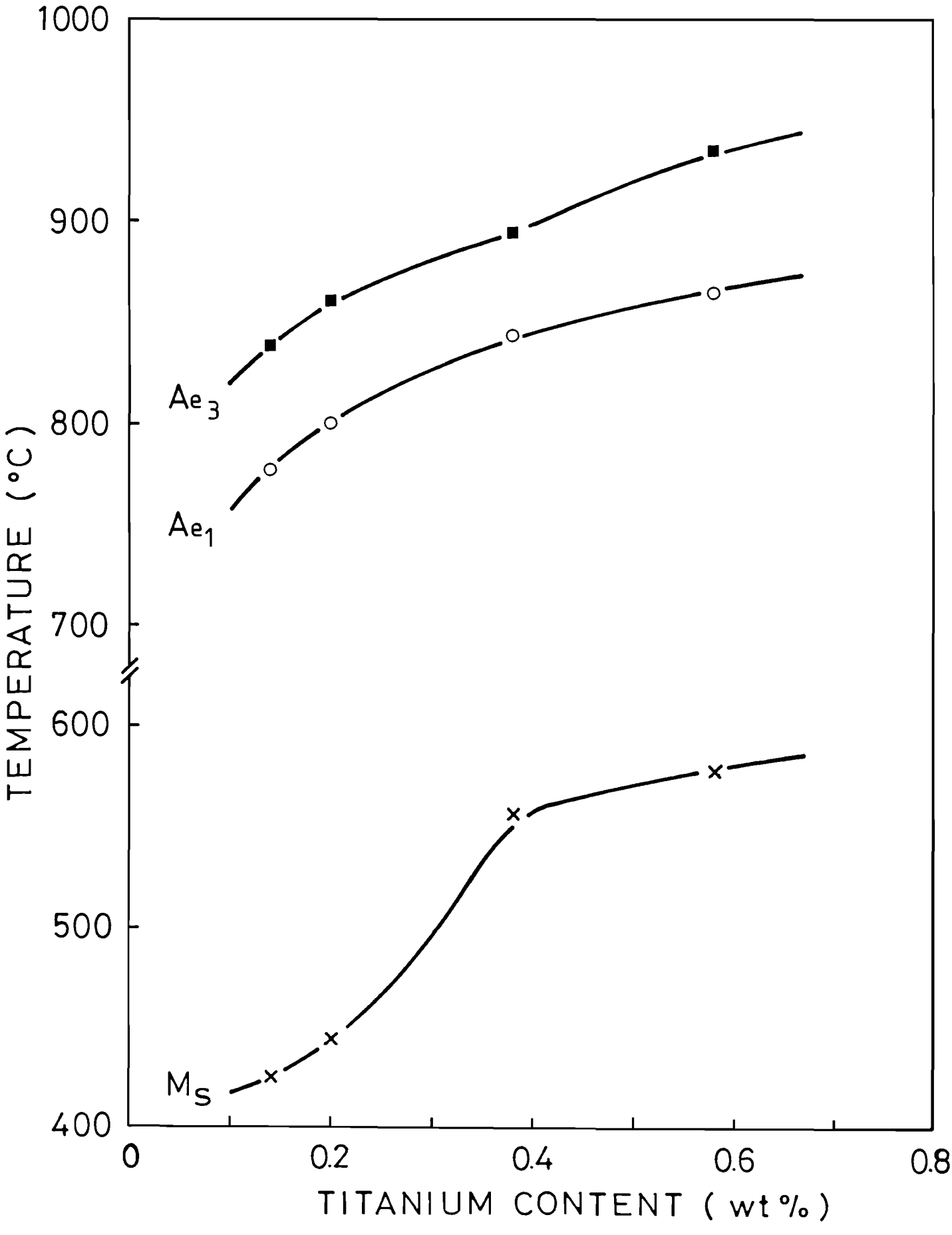

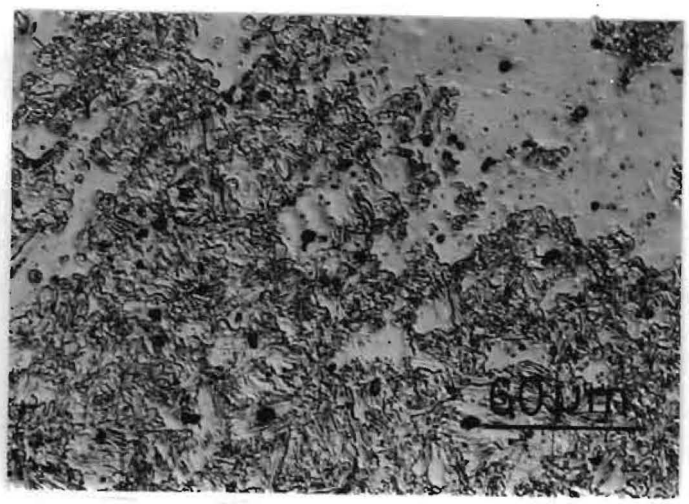

Sample 1 VPN: 199

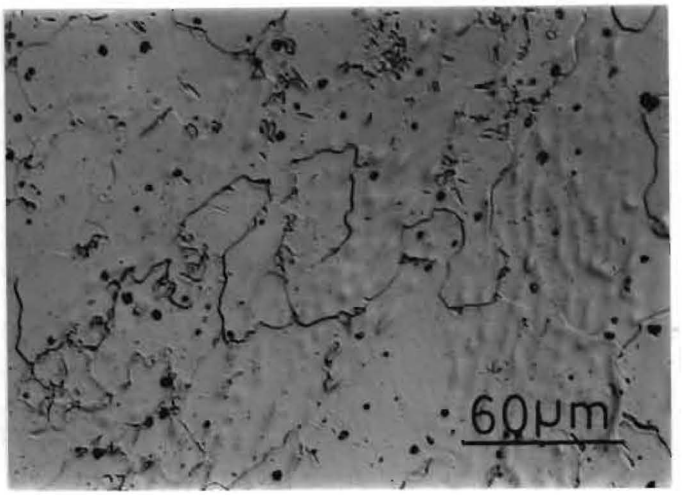

Sample 2 VPN: 140

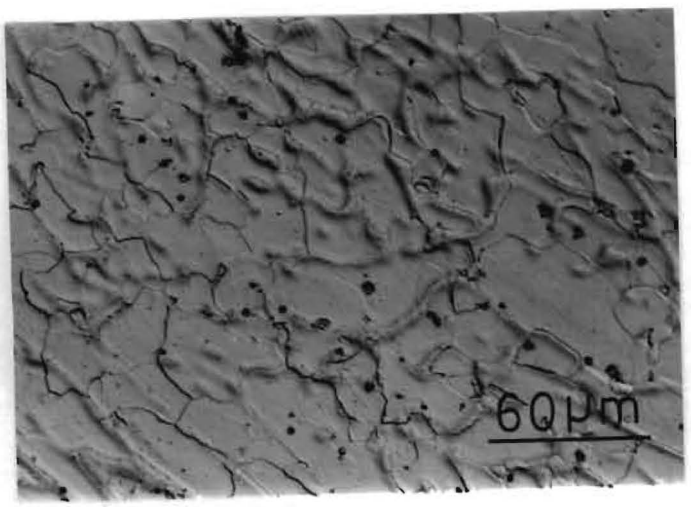

Sample 3 VPN: 142

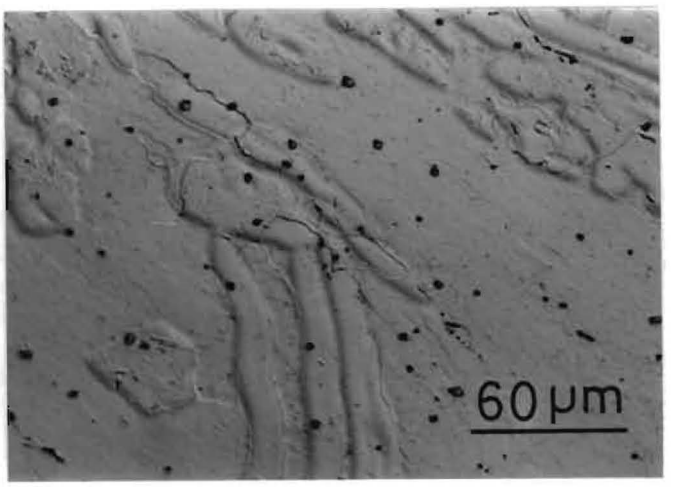

Sample 4 VPN: 143

Figure 4.21 Microstructure of titanium alloys, as-received condition.

CHAPTER 5 : DISCUSSION

5.1 The transformation temperatures of 3CR12

Although the dilation-temperature curve showed an austenite start-and finish-reaction, the latter did not necessarily imply that the specimen had become fully austenitic. The finish-reaction temperature may equally be that at which no new austenite was nucleated. The volume decrease associated with this transformation would then cease and the specimen would expand according to its thermal coefficient. The confirmatory anneals and associated tests showed that ferrite was present at temperatures abot the Ae_3 and that at temperatures sufficiently above this (1100^{o}C), delta ferrite became the dominant phase. Further confirmation was obtained during the austenitisation program which showed ferrite present in all the test specimens, although the reaction had gone to completion.

These results indicated that 3CR12 lies in the nose of the gamma loop of the Fe-Cr phase diagram (shown in Fig. 5.1). This would explain why 3CR12 never assumed a fully austenitic structure. However, the superimposition of this 3CR12 alloy on the phase diagram determined by Protopappas (1983) (Fig. 2.1), showed that it should be fully austenitic between 950^{o}C and 1100^{o}C. That this structure did not arise may be due to the different compositions, excluding nickel, that this alloy had to those which were used for the determination of the phase diagram. It will be shown in subsequent sections that 3CR12 is extremely sensitive to minor differences in alloy element concentrations and thus the apparent conflict between the present results and the existing phase diagram is explicable.

FIGURE 5.1.

IRON–CHROMIUM PHASE DIAGRAM

(from Metals Handbook, 1973)

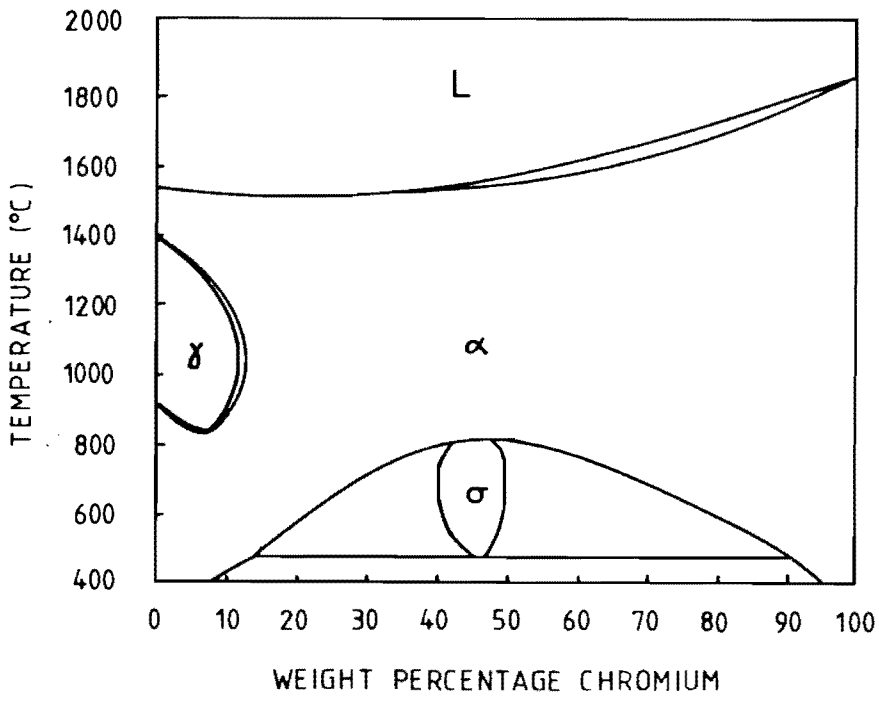

The high Ms temperature and the formation of martensite on furnace cooling is indicative of the high hardenability of 3CR12. This was expected due to the high chrome but low nickel and carbon contents of the steel. The high hardenability of 3CR12 signified that austenite is never present at room temperature. Therefore, the course of the various reactions must be followed by studying the martensite, and from this, inferring information about the prior austenite. This process is valid in terms of the characteristics of the martensite transformation, as discussed in Section 2.4, since the martensite grains inherit the composition, shape and size of the austenite from which it was formed. The strength of the resulting martensite is significantly altered, but this property is a function of the austenite from which it formed. The crystallographic relationship between the austenite and ferrite differs from that between the martensite and ferrite and therefore this information is lost during the transformation.

5.2 The austenite decomposition reaction (3CR12)

This transformation is not simply the decomposition of austenite since small quantities of ferrite (approximately 3%) are present in the starting structure. These discrete ferrite grains complicate the reaction as they offer alternative routes for the transformation. In a fully austenitic structure, ferrite should nucleate at austenite grain boundaries (see Section 2.1.2). When ferrite is present in the starting structure, two additional routes are feasible; either this ferrite could grow into the austenite with no new ferrite nucleating or additional ferrite could be sympathetically nucleated. The sympathetic nucleation of ferrite on growing grains is hindered because of the higher carbon concentrations in the surrounding austenite. This is due to the expulsion of carbon from the growing ferrite. With regard to the 3CR12 alloy under investigation, there are thus three possible modes of austenite decomposition, each of which may occur; the dominant mechanism will depend on the exact experimental conditions.

Since carbon is significantly less soluble in ferrite than it is in austenite, it must be expelled from solution on ferrite formation. In addition, nickel and manganese might partition between the austenite and the ferrite. It is, therefore, reasonable to assume that the ferrite growth, and possibly nucleation kinetics, are controlled by substitutional alloying element diffusion or carbon diffusion if the former do not partition. The mode of ferrite formation, however, could be controlled by the thermodynamic driving forces and not by diffusion.

From classical nucleation theory, the free energy change for homogeneous nucleation, ΔG, to form a nucleus of radius r, is

$$G = 4/3\pi r^3 \Delta G_B + 4\pi r^2 \gamma \qquad \text{(Verhoeven, 1975)}$$

where ΔG_B is the bulk free energy change on nucleation and γ is the surface free energy of the nucleus. The volume change associated with the nucleation event is assumed to be minimal and does not contribute a significant elastic term to the total free energy change. Furthermore, this term is constant for a constant nucleus size and morphology and it is independent of the nucleation site. For a nucleus to form, the decrease in the bulk, chemical free energy term must exceed the increase in the surface energy term. The effect of temperature on γ is small and γ can be taken as constant (Cottrell, 1957). The net surface energy term is significantly reduced on heterogeneous nucleation, whereby nucleation occurs on a pre-existing surface. The major factor in determining the difference in the driving force for the nucleation of the same phase at different temperatures, is thus the chemical free energy change, ΔG_B, associated with the transformation.

The driving force is the net gain in free energy arising from the transformation. This driving force will increase with an increasing difference between the transformation temperature and the equilibrium temperature (i.e. the temperature at which both phases have the same free energy), since the bulk free energy term increases without an associated increase in the surface energy. For the decomposition of austenite, the driving force increases with decreasing reaction temperature. It is therefore possible that the driving force at 700^{o}C for the formation of ferrite from austenite in 3CR12 is large enough to overcome the barriers to nucleation, whereas at 750^{o}C, the driving force is insufficient to cause the nucleation of new grains.

This does not preclude more ferrite from forming at 750^{o}C, rather the existing grains can grow into the surrounding matrix. If a new grain had nucleated around the existing grain and grown into the matrix

to the same extent that the existing grain had grown, the increase in surface energy would be equal to the surface energy of the original grain. Thus a greater driving force is required to nucleate a new grain than is required to grow an existing grain to the same size.

At 700^{o}C, the ferrite nucleation barriers are exceeded and new ferrite can nucleate and grow. This ferrite could nucleate at austenite grain boundaries, on defects within austenite grains or on ferrite-austenite grain boundaries. Intragranular nucleation can be discounted, since the grain boundaries provide faster paths for diffusion and are energetically more favourable nucleation sites (Section 2.1.2). The ferrite-ferrite boundaries are assumed to be coherent, since both crystals have the same BCC structure. This assumption is supported by Fig. 4.10 (a), where all three ferrite grains are simultaneously in the Bragg orientation. This is indicative of adjacent crystals having several lattice planes in common (Goux, 1974). This boundary would have a lower energy than the ferrite-austenite boundary and therefore constitutes a favourable nucleation site. Sympathetic nucleation would then be expected to dominate over the alternative austenite grain boundary sites.

Since carbon is effectively insoluble in ferrite but soluble in austenite, carbide precipitation must occur on the transformation to ferrite if the expelled carbon is not absorbed into solution by the austenite. On the isothermal decomposition of austenite, this precipitation would occur simultaneously with the growth of ferrite. Carbon supersaturation of ferrite should not occur because it would be expelled from solution on ferrite formation. The free carbon content of the alloy is low and therefore the austenite, during the early stages of the transformation, could absorb the carbon expelled by the ferrite. At later stages during the transformation, the carbon content of the austenite adjacent to the growing ferrite could reach a level whereby it is more preferable

for carbides to form, than it is for the austenite to dissolve more carbon. This could explain the observation that not all the ferrite grains which formed at 650°C and 700°C had significant quantities of precipitates.

The different types of carbide precipitates may be due to the nature of the migrating austenite-ferrite interface. The new ferrite was assumed to have a specific crystallographic relationship with the ferrite on which it nucleated and, therefore, would not have a specific relationship with the austenite grain into which it was growing. It is equally feasible that the original ferrite grain had a specific crystallographic (e.g. Kurdjumov-Sachs) relationship with one of its neighbouring austenite grains but no such relationship with its other neighbouring grains. That ferrite often has a Kurdjumov-Sachs relationship with an adjacent austenite grain is well documented, e.g. Honeycombe (1976). Different sympathetically nucleated growing grains would then have different relationships with their respective austenite grains and the nature of the interface would then be different, which could lead to different interface migration characteristics (Aaronson, 1974). This, in turn, could lead to different carbide morphologies, since the nature of the carbide is dependent on the boundary on which it formed.

At 750°C, ferrite growth was not extensive and the reaction rate was slow. Sufficient time was thus available for carbon diffusion through austenite, enabling the matrix to dissolve the carbon expelled by the ferrite. Consequently, carbon saturation of the austenite adjacent to the growing ferrite did not occur. This hypothesis provides a possible explanation for the lack of carbide deposition at 750°C.

The TTT curve (Fig. 4.11) for austenite decomposition of 3CR12 shows conventional "C" curve kinetics. This is typical of a nucleation and growth transformation for the isothermal decomposition

of a high temperature phase to a lower temperature stable phase. With an Ae_1 temperature of 792°C, a fully ferritic microstructure should result from the transformation at 750°C. The reaction, however, is shown as reaching completion without attaining this product. Considerable time would be necessary for this to occur, since the driving force at this temperature is small. After 16 hours the reaction had slowed to a negligible rate and can be considered to have effectively stopped.

5.3 The austenitisation reaction

A fully ferritic starting structure was used to enable the course of the reaction to be microstructurally monitored. If martensite had been present in the microstructure, either with ferrite or as the sole constituent, it would not have been possible to distinguish between this martensite and that which had formed from austenite during the transformation. The hardenability of 3CR12 is high, so any austenite formed will decompose to martensite on quenching.

The sigmoidal form of the isothermal transformation curves (Fig. 4.12) is consistent with the nucleation and growth mechanism observed microstructurally. The rate of the reaction was initially slow due to the gradual formation of stable nuclei, then accelerated with the growth of these nuclei and finally slowed down due to the impingement of neighbouring austenite growth regions. "C" curve kinetics did not occur; the reaction rate increased continually with increasing temperature (Fig. 4.13). This is typically due to the simultaneous increase in driving force and diffusion rates with increasing transformation temperature. The relative sluggishness of the reaction compared to previous studies e.g. Lenel (1980) and Law and Edmonds (1980) could be due to the low heating rates employed and the nature of the experimental apparatus i.e. bulk specimens transforming in air. This, however, provided a more

accurate simulation of the manufacturer's conditions.

The formation of grain boundary allotriomorphs is consistent with previously published results, see Section 2.2.3. The secondary sideplates and the convoluted interface of one side of the austenite (now martensite) grain in Fig. 4.15 (b) implied that the grains had nucleated with a specific crystallographic relationship with the ferrite. Due to the high hardenability of the steel, retained austenite was not present in the martensite lath structure. This prevented the confirmation and the nature of this crystallographic relationship from being obtained.

The sigmoidal nature of the transformation curves, the TTT curve and the nucleation and growth observed microstructurally, indicate that austenitisation in 3CR12 is a diffusion-controlled reaction. This is supported by the morphology of the austenite which formed during the reaction. The allotriomorphs initially grew along the grain boundaries in preference to growing into the ferrite grains. This may have occurred since diffusion along grain boundaries is faster than through the ferrite matrix. A similar explanation could be invoked for the lack of formation of intragranular idiomorphs and plates, since diffusion is faster along grain boundaries than along dislocations. The alloy elements which could control the diffusion kinetics can be divided into two groups: the interstitials, carbon and nitrogen or the substitutionals, nickel and manganese. On the basis of previous work (Aaronson and Domian, 1966 and Ball and Hoffman, 1981), the role of elements such as chromium and silicon can be discounted.

Since the hardness of martensite is primarily determined by the carbon and nitrogen levels and that the composition of the martensite is the same as the austenite from which it formed, hardness measurements provide a means of determining the change in interstitial composition of the austenite which formed during the transformation from ferrite. Such a plot was presented in

Fig. 4.16. The Fe-C phase diagram shows that the higher the transformation temperature in the dual phase austenite plus ferrite region, the less carbon will be in solution in the austenite at equilibrium, while above the Ae_3, the austenite can dissolve the same volume of carbon with increasing temperature. The resulting martensite formed from higher transformation temperatures should be softer than that formed from lower transformation temperatures and reach a constant value at temperatures above the Ae_3. This, however, was not observed, which discounts the effect that increasing transformation temperature may have played on the results. It can reasonably be assumed that any carbon in solution will be preferentially distributed in the austenite and not in the ferrite. At one transformation temperature, therefore, the more austenite formed, the lower the carbon content of each austenite grain and thus the softer should be the subsequent martensite. The reverse effect is evident for 3CR12. The sequence of the reaction must, therefore, be the formation of the austenite followed by the redistribution of the carbon. This is supported by the seemingly insignificant role that the carbides, present in the ferrite starting structure, played in the nucleation and growth of the austenite.

The diffusion kinetics must, therefore, be controlled by the nickel and manganese. The results of the electronprobe analysis (Table 4.3) indicate that both nickel and manganese partition to the austenite once it has formed. After 15 minutes at $860^{o}C$, the ratio of both elements in the austenite (now martensite) and ferrite was effectively one, whereas after 30 minutes, this ratio had increased significantly. This indicates that like carbon, the nickel and manganese partition to the austenite after its formation and are not directly involved in the transformation.

According to the Avrami equation for three-dimensional nucleation and growth processes, viz:

$$f = 1-\exp(-kt^{n})$$

a plot of $\log \log[1/(1-f)]$ against t, where f is the volume fraction transformed and t is the time should, for a diffusion controlled reaction, yield a straight line of slope n (Christian, 1975).

A curve of this nature for the transformation at 860°C is shown in Fig. 5.2. A straight line is not obtained. This confirms the analysis of the microprobe tests and microhardness measurements which indicated that the austenitisation reaction was not long range diffusion controlled.

From these results, it is apparent that the solute atoms and not alloying element diffusion kinetics provide the controlling mechanism for the reaction. Although long range diffusion gradients may be established due to the subsequent redistribution of the alloying elements, the dominant effect is the structural change from body centered cubic to face centered cubic. The change in crystal structure preceeds the redistribution of the nickel, manganese and carbon. From thermodynamic considerations (Lenel, 1980) neither carbon, nickel nor manganese need to partition between austenite and ferrite at transformation temperatures above the Ae_3. Unlike the decomposition reaction, where carbon must be expelled from the growing ferrite, the newly formed austenite can dissolve all the carbon that was in solution in the ferrite from which it formed. The redistribution need not, therefore, occur simultaneously with the structural change.

This suggests that the reaction proceeds via a Hultgren type para-equilibrium mechanism. The substitutional alloying element and the solvent participate in the change in crystal structure only. Their ratio is constant across the phase boundary which exists in a state of para-equilibrium. Unlike the decomposition reaction on which this mechanism was formulated, the kinetics are not controlled by carbon diffusion across the interface, but by the structural change alone. The reaction is controlled by processes at the interface and not by long range diffusion.

FIGURE 5.2.

KINETICS OF THE TRANSFORMATION FROM FERRITE TO AUSTENITE : 860°C

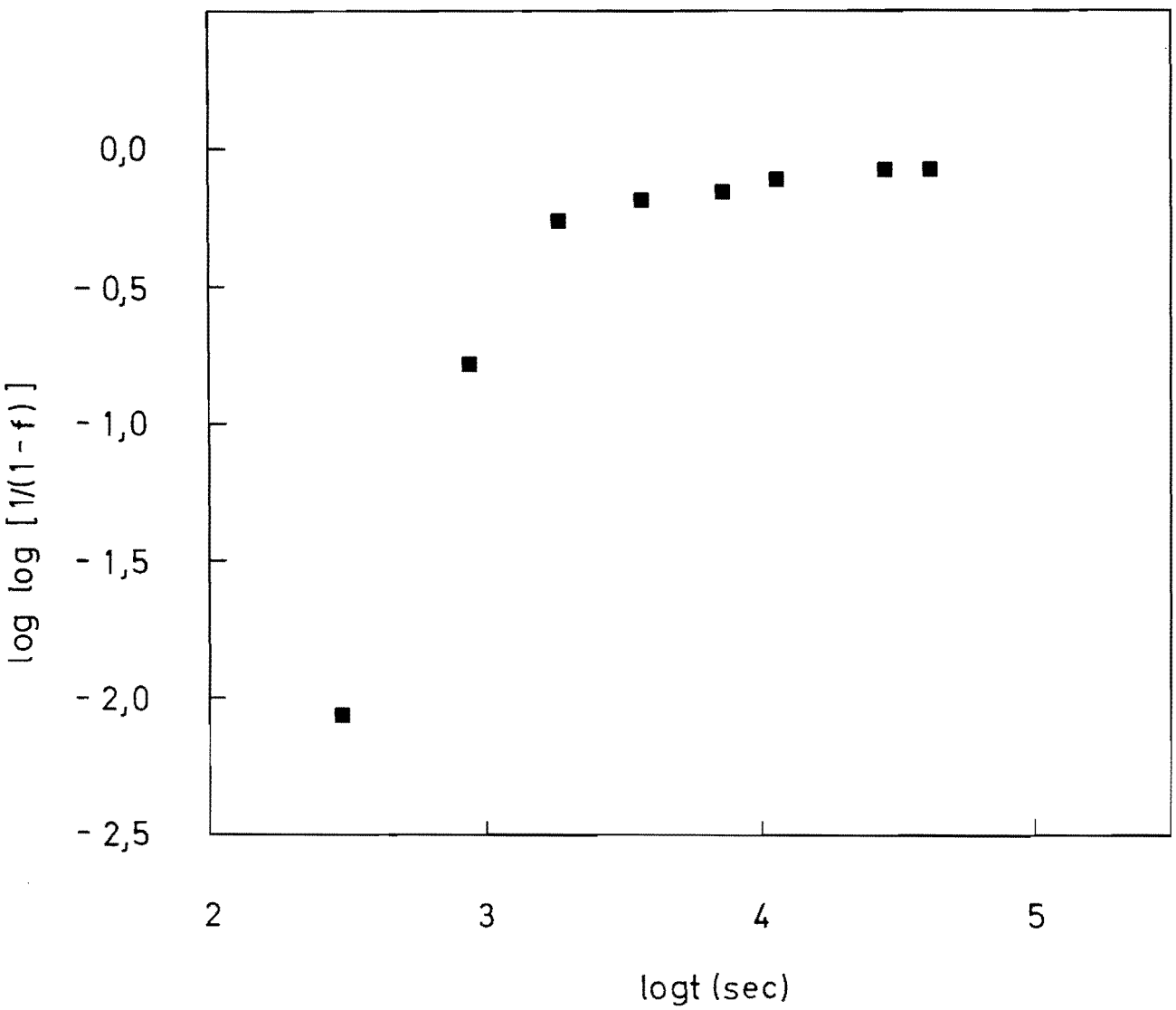

The "L" shape of the TTT curve cannot be explained by the simultaneous increase in driving force and diffusion rate, as was first suggested. The increased driving force at increased temperatures still applies, but since long range diffusion is not a controlling factor, this term obviously cannot influence the kinetics. Increasing the transformation temperature will not only increase the bulk free energy change associated with the reaction, but also increase the internal energy of each solute atom and hence facilitate the structural mutation.

5.4 3CR12Ni

The manufacturers had intended that the difference between the two alloys be related to the nickel content alone, 3CR12 having 0,67%Ni and 3CR12Ni having 1,21%Ni. However, the other alloying elements present in the steel also vary between the two materials, but only by small amounts. These disparities could be expected to influence certain characteristics of the steel, namely the extent of the various phase fields and the kinetics of the transformations between these fields.

The total austenite stabilising element content of 3CR12Ni is 2,18 wt% and of 3CR12 is 1,91 wt%. This value constitutes the sum of the carbon, nitrogen, nickel and manganese contents present in the respective steels. The total ferrite stabilising element content of 3CR12Ni and 3CR12 is 0,73 and 0,88 wt%, respectively. These values are the sum of the sulphur, phosphorous, silicon and titanium contents. The ratios of these austenite and ferrite stabilising values are 2,91 and 2,17 for 3CR12Ni and 3CR12, respectively.

The effect these elements have on the phase fields must be seen in terms of the Fe-Cr phase diagram, since chromium is the major alloying addition. The size of the gamma loop should, therefore, be enlarged to higher chromium levels and to lower temperatures.

3CR12Ni should have a lower Ae_1 temperature and might possibly fall entirely within the austenite region. Although the alloy does not become fully austenitic, small discreet ferrite grains remaining at temperatures above the Ae_3, the Ae_1 is $745^{o}C$, as opposed to $796^{o}C$ for 3CR12. The total alloying element concentration in the high nickel grade was also increased, which caused the drop in the Ms temperature by approximately 50^{o} to $389^{o}C$.

The austenite decomposition kinetics were retarded such that no reaction occurred on isothermal transformation at temperatures below the Ae_3. This is possibly as a result of the combined effect of lowering the austenite phase field and increasing the total alloy content with an associated decrease in the silicon content. All the alloying elements present, except silicon, are known to decrease the austenite decomposition kinetics (Aaronson and Domian, 1966). At $650^{o}C$, the lowest transformation temperature investigated, the alloy should become fully ferritic if the reaction is allowed to proceed for sufficient time. This temperature is 100^{o} below the Ae_1, the same margin at which ferrite was sympathetically nucleated in the low nickel grade. Assuming that the same thermodynamic arguments apply to both alloys, 3CR12Ni should follow the same trend as that exhibited by 3CR12. This did not occur because, as previously shown, the increased alloy content and the decreased Ae_1 temperature act together to decrease the diffusion kinetics of the rate controlling element(s).

A fully ferritic structure can be obtained in a specimen annealed at $650^{o}C$, since no structural change is necessary when the starting structure is the as-received condition, the martensite and ferrite of which are both body centered cubic (Ball and Hoffman, 1981). The only difference between the two phases is the increased lattice strains of the martensite and the preferential distribution of some of the elements to the martensite. The martensite to ferrite transformation will be a relaxation and recovery process. Neither

the growth of existing ferrite grains nor the nucleation of new grains is necessary. The high dislocation density of the martensite will add a new strain term to the bulk driving force, thus increasing the total free energy change associated with the reaction. The boundaries between the individual martensite laths will be eradicated and give way to ferrite grain boundaries, thus decreasing the overall interfacial area and the associated energy of the system. The disparity in the alloying element concentrations between the new ferrite and the old, pre-existing ferrite need not dissipate simultaneously with the recovery process for the transformation to occur; long range diffusion is not necessary.

5.5 The titanium effect

The presence of titanium in 3CR12 is particularly important due to its combination with carbon and nitrogen and the subsequent precipitation of titanium carbonitrides. Assuming that the TiC and TiN compounds form in stoichiometric proportions i.e. one mole of titanium reacts with one mole of carbon, and that all the available material combines, the amount of each element remaining in solution in each alloy will be:

Sample 1 : 0,002 wt%C + 0,002 wt% N
2 : 0,04 wt%Ti
3 : 0,32 wt%Ti
4 : 0,42 wt%Ti

It is well documented that carbon and nitrogen are strong austenitisers and that titanium is a strong ferritiser e.g. Honeycombe (1981). Carbon and nitrogen expand the austenite phase field, whereas titanium closes the field and restricts the formation of austenite. Consequently the more carbon and the less titanium in solution, the lower the temperature at which austenite will be stable. Increasing

the overall alloy content decreases the Ms temperature; carbon having the greatest effect of all the common alloying elements.

On this basis, and presuming that the elements had combined as indicated above, the Ae_1 and Ae_3 temperatures should increase continuously from specimen 1 to specimen 4. This is consistent with the observed results. Furthermore, sample 1 should have a lower Ms temperature than sample 2 since, in sample 1, carbon and nitrogen are present in an uncombined form in the matrix. The Ms temperature for sample 2 should be greater than that of samples 3 and 4 because there is a greater free alloying element content in the order 4>3>2 . The stoichiometrically predicted change in the Ms temperature has not been found; rather the Ms increases with increasing bulk titanium content. This suggests that in the four alloys all the titanium, but not all the carbon, was combined in the precipitates. However, the KEVEX micro-analysis (Table 4.7) showed free titanium present in all four specimens. The theoretically calculated free-alloy content levels, therefore, do not apply.

As the bulk titanium content is increased, there must be a simultaneous decrease in free carbon and an increase in free titanium levels, with free titanium and carbon present in all four alloys. This concomitantchange provides an explanation for the rise in all three transformation temperatures determined dilato-metrically. Decreasing the free carbon and increasing the free titanium will increase the temperature at which austenite is stable, while decreasing the extent of the austenite phase field. The rise in the Ms is indicative of the dominant role of carbon in controlling this temperature, since decreasing the free carbon content has a greater effect than increasing the free

titanium content. On addition of sufficient titanium, the Ms temperature should reach a maximum when the excess titanium overides the carbon response. This is not necessarily the point of zero free carbon. With further titanium additions the Ms should decrease.

As discussed above, increasing the bulk titanium content decreases the extent of the austenite phase field. This is due to the removal of carbon from, and the addition of titanium to solution. Both invoke the same response on the austenite region, giving the titanium a dual effect. If this is applied to the iron-chromium phase diagram, some effect should be seen in the relative position of the gamma loop . Increasing the bulk titanium content would decrease the size of this loop and shift the nose to lower chromium levels. Depending on the extent of this movement, 3CR12, with a constant chromium content, could be displaced so as to lie either within the fully austenitic region or to avoid the loop altogether and remain fully ferritic from room temperature to the liquidus temperature.

Dilatometry indicated that a ferrite to austenite transformation occurred in all four alloys, thereby showing that the austenite phase field had not been reduced sufficiently, even in the high titanium case, for the alloy to be fully ferritic at all temperatures. Dilatometry, however, cannot indicate the extent of the austenite reaction. To determine if the expansion of the austenite region, at the lowest titanium levels, was sufficient to cause a complete austenitisation transformation, specimen 1 was annealed for 1 hour at 100^{o}C above its Ae_3 temperature. The alloy did not become fully austenitic but the volume fraction of the ferrite was reduced to 0,01. The gamma loop had been displaced relative to the bulk chromium content, but by an amount that was insufficient to cause the formation of 100% austenite.

5.6 Overview

Although this study was chiefly an academic exercise it is applicable to the manufacture of 3CR12. The TTT curves were not intended to be directly related to specific industrial processes but may be used as a guide in the design of the manufacturing conditions. The constraints placed on the system, namely the nature of the apparatus and the specific thermal conditions, prevent the direct commercial use of the results. The methods were chosen so as to enable the reaction paths to be followed and the governing factors to be determined. The realisation of this aim, however, prevented the accurate modelling of the manufacturing process. For example, a fully ferritic microstructure was used as the starting condition for the austenitisation program. The manufacturers, however, will intercritically anneal the steel from the hot rolled condition which consists of martensite and stringers of ferrite. The morphology of the resulting austenite and hence the final martensitic structure will be different to those found experimentally. The kinetics of the industrial anneal will also be altered. The results presented in this dissertation provide an approximate reaction time scale and a better understanding of the nature of the process and can therefore serve as a guide to the manufacturer.

An important factor to emerge from this program is the critical control of the alloying element content necessary for the manufacture of a standard product. This is especially important in terms of the carbon and titanium levels since these elements act in tandem and exert a significant influence on the outcome of the final microstructure. Since both elements are only present in small amounts, minor fluctuations in composition represent major percentage changes. An increase in the carbon content with a simultaneous decrease in the titanium content, influences the structure to a greater extent than if just the carbon content was

increased. These modifications to the composition serve to alter the size and position of the gamma loop in the Fe-Cr phase diagram. Thus, different structures can result from the same heat treatment of two poorly controlled batches of the same basic steel.

CHAPTER 6 : CONCLUSIONS

The objectives of this study were the determination of the TTT diagrams for the reactions between ferrite and austenite in 3CR12 and an investigation into the factors controlling these transformations. The objectives also included an investigation into the decomposition of austenite in a high nickel alloy, 3CR12Ni, and the effect that varying titanium content had on the Ms, Ae_1 and Ae_3 temperatures of 3CR12. It was intended that this work would aid the producers of 3CR12 in optimising their manufacturing conditions in order to improve the in-service performance of the steel. This study has led to the following conclusions:

(1) The 3CR12 alloy used in this study did not become fully austenitic; small ferrite grains were present at temperatures above the Ae_3. This implied that, with respect to the Fe-Cr phase diagram, the alloy on heating, passed through the nose of the gamma loop.

(2) Since a fully austenitic structure was never achieved, the phase transformation from temperatures above the Ae_3 to below the Ae_1 was not simply the decomposition of austenite. Two temperature regimes were identified: (a) at 750°C, the existing ferrite grains grew into the austenite matrix and (b) at 650°C and 700°C, new ferrite was sympathetically nucleated, that is, it was heterogeneously nucleated on existing ferrite/austenite grain boundaries. The different mechanisms were due to the different driving forces existing in the two regimes. At the lower temperatures the driving force was sufficient to overcome the additional grain boundary energy created by the nucleation of the new grains.

(3) At 650°C and 700°C, two types of carbide precipitation occurred in the ferrite. These were (a) random precipitation within the grain and (b) interphase precipitation. The two modes were due to the different austenite/ferrite boundary configurations and migration mechanisms existing at different interfaces.

(4) The TTT diagram for the decomposition of austenite showed conventional "C" curve kinetics. This arose from the simultaneous increase in the thermodynamic driving force and decrease in the diffusion rates on decreasing transformation temperature.

(5) The austenitisation reaction occurred by a Hultgren type para-equilibrium mechanism. The rate controlling process was the structural change from the body centered cubic crystal structure of ferrite to the face centered cubic crystal structure of austenite. The reaction was not long range diffusion controlled; the partitioning of the Ni, Mn and C to the austenite occurred after the crystal structure had changed.

(6) The kinetics of the ferrite to austenite reaction increased continuously with increasing transformation temperature. Increasing the transformation temperature increased both the driving force for the reaction and the energy of each individual atom. This led to the "L" shape of the TTT curve.

(7) No growth of ferrite occurred on the isothermal transformation of 3CR12Ni at temperatures below the Ae_1 because the increased alloy element concentration of this alloy, compared with 3CR12, decreased the Ae_1 temperature. Hence the diffusion kinetics of the rate controlling elements were decreased. A martensite to ferrite transformation could occur since no structural change or diffusion was necessary.

(8) Increasing the bulk titanium content increased the Ms, Ae_1 and Ae_3 temperatures of 3CR12 due to the removal of carbon from, and the addition of titanium to, solution. The size of the gamma loop decreased with increasing bulk titanium, which also shifted the loop to lower temperatures and lower chromium concentrations. Neither all the titanium nor all the carbon was combined in the Ti(CN) precipitates which formed.

(9) The TTT curves determined illustrate the nature of the reaction kinetics and indicate the approximate rates at which the various transformations occur. They may be used as a guide in the production of 3CR12, but the exact manufacturing conditions cannot be directly extrapolated from them.

(10) This work has shown the importance of precise control of composition, which is necessary for the production of a uniform 3CR12 product.

REFERENCES

Aaronson, H.I. (1974) : "Observations on interphase boundary structure", J. Microscopy, 102, 3, pp 275-300.

Aaronson, H.I. and Domian, H.A. (1966) : "Partition of alloying elements between austenite and proeutectoid ferrite or bainite", Trans. Met. Soc. AIME, 236, pp 781-796.

Aaronson, H.I., Domian, H.A. and Pound, G.M. (1966) : "Thermodynamics of the austenite-proeutectoid ferrite transformation; II, Fe-C-x alloys", Trans. Met. Soc. AIME, 236, pp 768-781.

Aaronson, H.I., Laird, C. and Kinsman, K.R. (1970) : "Mechanisms of diffusional growth of precipitate crystals", Phase Transformations, H.I. Aaronson, ed, ASM, pp 313-393.

Aaronson, H.I. and Wells, C. (1956) : "Sympathetic nucleation of ferrite", J. Metals, 8, pp 1216-1223.

Albutt, K.J. and Garber, S. (1966) : "Effect of heating rate on the elevation of the critical temperatures of low-carbon mild steel", JISI, 204, pp 1217-1222.

Apple, C.A., Caron, R.N. and Krauss, G. (1974) : "Packet microstructure in Fe-0,2pct C martensite", Met. Trans., 5, pp 593-599.

Ball, A. and Hoffman, J.P. (1981) : "Microstructure and properties of a steel containing 12% Cr", Metals Technology, 8, 9, pp 329-338.

Batte, A.D. and Honeycombe, R.W.K. (1973) : "Precipitation of vanadium carbide in ferrite", JISI, 211, pp 284-289.

Beraha, E. and Shpigler, B. (1977) : "Color Metallography", ASM, Metals Park, Ohio.

Berry, F.G. and Honeycombe, R.W.K. (1970) : "The isothermal decomposition of austenite in Fe-Mo-C alloys", Met. Trans., 1, pp 3279-3286.

Brink, A.B. (1982) : "The high temperature mechanical properties of 3CR12Ni", Internal Report, University of Cape Town.

Chilton, J.M. and Kelly, P.M. (1968) : "The strength of ferrous martensite", Acta Met., 16, pp 637-656.

Christian, J.W. (1975) : "The theory of transformations in metals and alloys", 2nd edition, Part 1, Pergamon Press, Oxford.

Coates, D.E. (1973) : "Diffusional growth limitation and hardenability", Met. Trans., 4, pp 2313-2325.

Coldren, A.P. and Eldis, G.T. (1980) : "Using CCT diagrams to optimise the composition of an as-rolled dual phase steel", J. Metals, 32, 3, pp 41-48.

Cottrell, A.H. (1957) : "Theoretical structural metallurgy", 2nd edition, Edward Arnold, London.

Davenport, A.T. and Honeycombe, R.W.K. (1971) : "Precipitation of carbides at γ-α boundaries in alloy steels", Proc. Roy. Soc. London, A322, pp 191-205.

Davies, R.G. (1978) : "The deformation behaviour of a vanadium strengthened dual phase steel", Met. Trans. A, 9A, pp 41-52.

Demo, J.J. (1977) : "Structure and constitution of wrought ferrite stainless steels", "Handbook of Stainless Steels", D. Peckner and I.M. Bernstein, eds., McGraw-Hill, New York.

Dubé, C.A. (1948) : Ph.D. Thesis, Carnegie Institute of Technology, cited in Aaronson et al (1970).

Fong, H.A. and Glover, S.G. (1975) : "Some factors influencing morphology of grain boundary austenite precipitates formed during nitriding of Fe-1,93% Mn at 645°C", Trans.Japanese Institute of Metals, 16, pp 115-122.

Garcia, C.I. and De Ardo, A.J. (1979) : "The formation of austenite in low-alloy steels", "Structure and properties of dual phase steels", Proc. AIME Symposium, New Orleans, J.W. Morris Jr. and R. Kot, eds., pp 40-61.

Goux, C. (1974) : "Observation of grain boundaries", J. Microscopy, 102, 3, pp 241-260.

Grozier, J.D., Paxton, H.W. and Mullins, W.W. (1965) : "The growth of austenite into ferrite in the iron-nitrogen system", Trans. Met. Soc. AIME, 233, pp 130-142.

Heikkinen, V.K. (1973) : "The formation of planar band colonies in vanadium-bearing mild steels", Acta Met., 21, pp 709-714.

Hillert, M., Nilsson, K. and Torndahl, L.-E. (1971) : "Effect of alloying elements on the formation of austenite and dissolution of cementite", JISI, 209, pp 49-66.

Hilliard, J.E. (1968) : "Measurement of volume in volume", "Quantitative Microscopy", R.T. De Hoff and F.N. Rhines, eds., McGraw-Hill, New York.

Hilliard, J.E. and Cahn, J.W. (1961) : "An evaluation of procedures in quantitative metallography for volume fraction analysis", Trans. Met. Soc. AIME, 221, pp 344-352.

Hoffman, J.P. (1982) : personal communication.

Honeycombe, R.W.K. (1976) : "Transformation from austenite in alloy steels", Met. Trans. A, 7A, 7, pp 915-936.

Honeycombe, R.W.K. (1979) : "Some aspects of the γ-α transformation in alloy steels", Phase Transformations, Series 3, 1, 11, pp 19-26.

Honeycombe, R.W.K. (1981) : "Steels", Edward Arnold, London.

Hultgren, A. (1947) : "Isothermal transformation of austenite", Trans. ASM, 39, pp 915-1005.

Irvine, K.J., Crowe, D.J. and Pickering, F.B. (1979) : "The physical metallurgy of 12% chromium steels","The Metallurgical Evolution of Stainless Steels", F.B. Pickering, ed., ASM, Metals Park, Ohio.

Judd, R.R. and Paxton, H.W. (1968) : "Kinetics of austenite formation from a spheroidized ferrite-carbide aggregate", Trans. Met. Soc. AIME, 242, pp 206-215.

Kehoe, M. and Kelly, P.M. (1970) : "The role of carbon in the strength of ferrous martensite", Scripta Met., 4, pp 473-476.

Kinsman, K.R. and Aaronson, H.I. (1973) : "Influence of Al, Co and Si upon the kinetics of the proeutectoid ferrite reaction", Met. Trans., 4, pp 959-967.

Koch, F. and Eckstein, M.J. (1978) : "Studies of the redistribution of chrome and nickel during the ferrite to austenite transformation in chrome-nickel steels of the 26-6 type", Steel Furnace Monthly, 13, 11, pp 441-445.

Krauss, G. and Marder, A.R. (1971) : "The morphology of martensite in iron alloys", Met. Trans., 2, pp 2343-2357.

Law, N.C. and Edmonds, D.V. (1980) : "The formation of austenite in a low alloy steel", Met. Trans. A, 11A, pp 33-46.

Lenel, U.R. (1980) : "Reaustenitisation of some alloy steels", Ph.D. Thesis, University of Cambridge.

Leone, G.L. and Kerr, H.W. (1982) : "The ferrite and austenite transformation in stainless steels", Welding Journal, 61, 1, pp 13s-21s.

Lula, R.A. (1977) : "Residual and minor elements in stainless steel", "Handbook of Stainless Steels", D. Peckner and I.M. Bernstein, eds., McGraw-Hill, New York.

Marder, A.R. (1982) : "Deformation characteristics of dual phase steels", Met. Trans. A, 13A, pp 85-92.

Martin, D. (1981) : "3CR12 developement work", Internal Report, Middelburg Steel and Alloys (Pty) Ltd.

Matsuda, S. and Okamura, Y. (1974a) : "Microstructural and kinetic studies of reverse transformation in low-carbon low-alloy steel", Trans. ISIJ, 14, pp 363-368.

Matsuda, S. and Okamura, Y. (1974b) : "The later stages of reverse transformation in low-carbon low-alloy steels", Trans. ISIJ, 14, pp 444-449.

Melvill, M.L., Mahony, C.S., Hoffman, J.P. and Dewar, K. (1980) : "The development of a chromium-containing corrosion resisting steel", Proc. Conf. Third South African Corrosion Conference.

Metals Handbook, 8th edition, 8, ASM, Metals Park, Ohio, 1973.

Molinder, G. (1956) : "A quantitative study of the formation of austenite and the solution of cementite at different austenitising temperatures for a 1,27% carbon steel", Acta Met., 4, pp 565-571.

Nemoto, M. (1977) : "The formation of austenite from mixtures of ferrite and cementite as observed by HVEM", Met. Trans. A, 8A, pp 431-437.

Noël, R.E.J. (1981) : "The abrasive-corrosive wear behaviour of metals", M.Sc. Thesis, University of Cape Town.

Novak, C.J. (1977) : "Structure and constitution of wrought austenite stainless steels", Handbook of Stainless Steels, D. Peckner and I.M. Bernstein, eds., McGraw-Hill, New York.

Owen, W.S. (1980) : "Can a simple heat treatment help to save Detroit?", Metals Technology, 7, pp 1-13.

Pavlick, J.E., Mullins, W.W. and Paxton, H.W. (1966) : "The growth of nitrogen-austenite into alloyed ferrite", Trans. Met. Soc. AIME, 236, pp 875-881.

Pickering, F.B. (1978) : "Physical metallurgy and the design of steels", Applied Science, London.

Pickering, F.B. (1979) : "Some aspects of the heat treatment of welded corrosion and heat resisting steels","The Metallurgical Evolution of Stainless Steels", F.B. Pickering, ed., The Metals Society, London.

Plitcha, M.R. and Aaronson, H.I. (1974) : "Influence of alloying elements upon the morphology of austenite formed from martensite in Fe-C-X alloys", Met. Trans., 5, pp 2611-2613.

Protopappas, E. (1983) : M.Sc. Thesis, University of Cape Town.

Rashid, M.S. (1981) : "Dual phase steels", Ann. Rev. Mat. Sci., 11, pp 245-266.

Ricks, R.A., Bee, J.V. and Howell, P.R. (1981) : "The decomposition of austenite in a high purity iron-chromium-nickel alloy", Met. Trans. A, 12A, pp 1587-1594.

Ricks, R.A. Howell, P.R. and Honeycombe, R.W.K. (1979) : "The effect of Ni on the decomposition of austenite in Fe-Cu alloys", Met. Trans. A, 10A, pp 1049-1058.

Roberts, G.A. and Mehl, R.F. (1943) : "The mechanism and the rate of formation of austenite from ferrite-cementite aggregates", Trans. ASM, 31, pp 613-649.

Sondenbergh, R. (1980) : "Research on 3CR12 - University of Pretoria", Internal Report, Middelburg Steel and Alloys (Pty) Ltd.

Speich, G.R. and Szirmae, A. (1969) : "Formation of austenite from ferrite and ferrite-carbide aggregates", Trans. Met. Soc. AIME, 245, pp 1063-1074.

Speich, G.R. and Warlimont, H. (1968) : "Yield strength and transformation substructure of low-carbon martensite", JISI, 206, pp 385-392.

Steigerwald, R.F., Dundas, H.J., Redmond, J.D. and Davison, R.M. (1979) : "The physical metallurgy of Fe-Cr-Mo ferritic stainless steel", "The Metallurgical Evolution of Stainless Steel", F.B. Pickering, ed., The Metals Society, London.

Thomas, G. (1971) : "Electron microscopy investigations of ferrous martensites", Met. Trans., 2, pp 2373-2385.

Underwood, E.E. (1970) : "Quantitative Stereology", Addison-Wesley, Reading, Massachusetts.

Verhoeven, J.D. (1975) : "Fundamentals of physical metallurgy", John Wiley and Sons, New York.

Walker, D.H. (1982) : personal communication.

Wycliffe, P.A., Purdy, G.R. and Embury, J.D. (1981) : "Growth of austenite in the intercritical annealing of Fe-C-Mn dual phase steels", Can. Met. Q., 20, 3, pp 339-350.